Sage Journals

Toxicologic Pathology

Impact Factor: **1.4**
5-Year Impact Factor: **1.9**



## Abstract

Air pollution is a serious environmental problem. We investigated whether residency in cities with high air pollution is associated with neuroinflammation/neurodegeneration in healthy children and young adults who died suddenly. We measured mRNA cyclooxygenase-2, interleukin-1β, and CD14 in target brain regions from low (n = 12) or highly exposed residents (n = 35) aged 25.1 ± 1.5 years. Upregulation of cyclooxygenase-2, interleukin-1β, and CD14 in olfactory bulb, frontal cortex, substantia nigrae and vagus nerves; disruption of the blood-brain barrier; endothelial activation, oxidative stress, and inflammatory cell trafficking were seen in highly exposed subjects. Amyloid β42 (Aβ42) immunoreactivity was observed in 58.8% of apolipoprotein E (APOE) 3/3 < 25 y, and 100% of the APOE 4 subjects, whereas α-synuclein was seen in 23.5% of < 25 y subjects. Particulate material (PM) was seen in olfactory bulb neurons, and PM < 100 nm were observed in intraluminal erythrocytes from lung, frontal, and trigeminal ganglia capillaries.

Exposure to air pollution causes neuroinflammation, an altered brain innate immune response, and accumulation of Aβ42 and α-synuclein starting in childhood. Exposure to air pollution should be considered a risk factor for Alzheimer's and Parkinson's diseases, and carriers of the APOE 4 allele could have a higher risk of developing Alzheimer's disease if they reside in a polluted environment.

## Introduction

Air pollution is a complex and dynamic mixture of gases, particulate matter (PM), and organic compounds present in outdoor and indoor air. Exposure to air pollution is associated with respiratory, cardiovascular, and stroke-related sickness and death (Banauch et al. 2006; Brunekreef and Holgate 2002). Children living in Mexico City (MC) exhibit evidence of chronic inflammation of the upper and lower respiratory tracts, alterations in circulating inflammatory mediators, and breakdown of the nasal epithelial barrier (Calderón-Garcidueñas et al. 2001; Calderón-Garcidueñas, Franco-Lira et al. 2007; Calderón-Garcidueñas, Mora-Tiscareño et al. 2003). These children also have heart rhythm alterations and decreased vagal responses associated with sustained high plasma endothelin-1, a potent vasoconstrictor peptide involved in the homeostatic regulation of vascular smooth muscle tone, and upregulated after exposure to air pollutants including PM (Thomson et al. 2004, 2005; Calderón-Garcidueñas et al. 2006; Calderón-Garcidueñas, Vincent et al. 2007). Dogs exposed to the polluted environment in MC exhibit chronic respiratory tract inflammation; early expression of neuronal nuclear NFκB and endothelial/glial inducible nitric oxide synthase; disruption of the nasal and olfactory barriers and the blood-brain barrier (BBB); accumulation of amyloid β42 (Aβ42) in neurons; and increased olfactory bulb (OB) and hippocampal apurinic/apyrimidinic sites, indicators of oxidative DNA damage (Calderón-Garcidueñas et al. 2001, 2002; Calderón-Garcidueñas, Maronpot et al. 2003). Breakdown of the nasal respiratory and olfactory epithelium and the BBB facilitates the access of systemic inflammatory mediators and components of air pollution to the central nervous system (CNS) (Calderón-Garcidueñas et al. 2004). Chronic inflammatory processes in the CNS play an important role in the progressive neuronal death seen in neurodegenerative diseases such as Alzheimer's (Akiyama et al. 2000; McGeer et al., 2006; Selkoe 2001, 2002). A coherent pathway linking exposure to air pollution and brain damage includes a chronic inflammatory process involving the respiratory tract, which results in a systemic inflammatory response with the production of inflammatory mediators capable of reaching the brain; continuous expression of crucial inflammatory mediators in the CNS at low levels; and the formation of reactive oxygen species (ROS) (Calderón-Garcidueñas et al. 2002, Calderón-Garcidueñas et al. 2004; Calderón-Garcidueñas, Maronpot et al. 2003; Calderón-Garcidueñas, Mora-Tiscareño et al. 2003). Ultrafine PM (UFPM), particulate-matter–associated lipopolysaccharides (PM-LPS), and metal uptake could take place through olfactory neurons, cranial nerves such as the trigeminal and vagus, the systemic circulation, and macrophage-like cells loaded with PM from the lungs (Calderón-Garcidueñas et al. 2001, 2002; 2004; Calderón-Garcidueñas, Maronpot et al. 2003; Calderón-Garcidueñas, Mora-Tiscareño et al. 2003). Activation of the brain innate immune responses could follow the interaction between circulating cy

and constitutively expressed cytokine receptors located in endothelial brain capillary cells, followed by activation of cells involved in adaptive immunity (Nguyen et al. 2002; Simard and Rivest 2006). Monocytes are the main innate immune response mediator cells, producing and secreting TNFα, IL-6, and interleukin-1β (IL-1β), which in turn recruit and increase the activity of other immune cells (Simard and Rivest 2006). In the sustained upper and lower respiratory tract chronic inflammatory process elicited on exposure to significant concentrations of air pollutants in megacities such as MC, particularly fine and ultrafine PM could serve as the crucial trigger for a chain of events leading to endothelial activation, disruption of the BBB, altered response of the innate immune system, neuroinflammation, and neurodegeneration. We previously reported that adult residents of highly polluted urban areas, average age 54.7 ± 4.8 years, exhibit significantly higher expression of cyclooxygenase-2 (COX2)—a powerful inflammatory gene—in brain target areas when compared with matched age/gender/educational level subjects from cities with low pollution levels (Calderón-Garcidueñas et al. 2004). Highly exposed subjects also exhibited a significant neuronal and astrocytic accumulation of the 42 amino acid-isoform (Aβ42) of β amyloid, which is more hydrophobic and prone to aggregation than other Aβ isoforms (Selkoe 2001, 2002). Given that pollutant levels in MC vary within a relatively narrow range throughout the year, its residents are exposed all year long to a significant burden of air pollutants. The pollution levels have been sustained or have worsened in the past twenty years (Bravo-Alvarez and Torres-Jardón 2002), so the exposure of today's children and teenagers is truly life long, as it began in utero. Moreover, there is a relatively low mobility of MC residents, so individuals tend to be exposed to the same environment for long periods, thus allowing for the opportunity to study chronic health effects associated with prolonged sustained exposure to severe air pollution.

The primary purpose of the present work was to measure by real-time polymerase chain reaction two key inflammatory genes, COX2 and IL-1β, and the LPS receptor CD14; this selection was based on the increasing evidence that neuroinflammatory processes contribute to the cascade of events that lead to neurodegeneration. These markers of neuroinflammation were measured in target brain areas including the OB, frontal cortex, hippocampus, substantia nigrae, periaqueductal gray, and vagus nerves in a cohort of cognitively intact Mexican children, adolescents, and young adults who died suddenly and were residents from low- or high-polluted urban areas in Mexico. Given that inflammatory responses involve the microvasculature and the trafficking of inflammatory cells, we also explore the integrity of the tight junctions in the brain capillaries, the nature of the

inflammatory responsive cells, and the expression of endothelial inflammatory markers. We assessed zonula occludens-1 (ZO-1), a scaffolding protein marking tight and adherens junctions. Immune cells were identified immunohistochemically using antibodies to CD68, surface HLA-DR antigens, and CD163 (a macrophage scavenger receptor that identifies brain perivascular macrophages). Leukocyte adhesion molecules investigated included vascular adhesion molecule-1 (VCAM-1), and intercellular adhesion molecule-1 (ICAM-1). Since we have seen the transfer of UFPM from alveolar type I cells to the alveolar epithelial basement membrane, to endothelial cells, and finally to macrophage-like cells in the lumen of exposed MC dog lung capillaries (Calderón-Garcidueñas et al. 2001; Calderón-Garcidueñas, Franco-Lira et al. 2007), we did extensive electron microscopy in samples from the lungs and brains of both control and exposed MC subjects to look for PM. The accumulation of Aβ42 and α-synuclein was also investigated. The trigeminal ganglia were examined given the evidence by Lewis et al. of trigeminal uptake and clearance of inhaled manganese in rodents. In addition, the cohorts were genotyped for the APOE alleles and allelic frequencies of the Asp299Gly TLR4 polymorphism to determine if subjects had a known risk factor for Alzheimer's disease (i.e., APOE ε4 allele carriers) and if they were capable of responding to lipopolysaccharides (one of the major organic components in MC PM).

## Methods

### Study Cities and Air Quality Data

We selected a large, polluted megacity and two control cities. Mexico City (MC) was the selected megacity, and Tlaxcala and Veracruz were the low-polluted cities. Mexico City represents an extreme of urban growth and environmental pollution (Bravo-Alvarez and Torres-Jardón 2002). Mexico City is a megacity that covers an area of 2000 $km^2$ surrounded by a series of volcanic and discontinuous mountain ranges that limit the natural ventilation of the basin. The basin has more than 30,000 industrial facilities and 4 million vehicles, with an estimated annual emission of 2.6 million tons of particulate and gaseous air pollutants. The critical air pollutants are ozone ($O_3$), and PM. The climatic conditions in MC are relatively stable through the seasons, thus air pollutant concentrations are relatively consistent. Residents in MC have been chronically exposed to significant concentrations of $O_3$, PM, and LPS for the past 2 decades. The marked increase in $O_3$ concentrations initially started in the fall of 1986, coinciding with the introduction of a new gasoline with lower tetraethyl lead concentration and higher levels of short-chain aliphatic hydrocarbons and aromatic

compounds (Bravo-Alvarez and Torres-Jardón 2002). The change in gasoline composition led to an increase in reactive hydrocarbon emissions and $O_3$ ambient concentrations. By the end of 1989, in an apparent move to further reduce atmospheric carbon monoxide and hydrocarbon emissions, methyl-ter-butyl ether (MTBE) was introduced as an additive in gasoline. However, the use of MTBE in the absence of catalytic converters on motor vehicles led to a further increase in reactive hydrocarbons (i.e., isobutene and formaldehyde). As a result, $O_3$ production chemistry changed, leading to an additional rise in ambient $O_3$ concentrations. Around the same time, MC authorities imposed a regulation banning residents from driving cars on specific days of the week. This measure significantly increased total driving in MC, because many people bought an additional car because of the inefficient public transportation. The resulting effect of the greater use of old cars not equipped with catalytic converters, overcrowded streets, and increased weekend driving was a serious boost in vehicular emissions, which, combined with the use of MTBE in gasoline, led to very high $O_3$ levels that peaked in 1991 (Bravo-Alvarez and Torres-Jardón 2002). Citizen concerns about air pollution and car market pressure to introduce new cars equipped with catalytic converters forced authorities to consider the distribution of reformulated gasoline free of tetraethyl lead. As a consequence, beginning with 1991 car models, catalytic converters were required in Mexico, although the turnover rate to new converter-equipped cars was slow because of the weak economic situation. A slight reduction in $O_3$ ambient levels started in 1992. Additional measures, such as the vehicle emission inspection program and more strict control of hydrocarbon emissions from gas stations, helped to reduce $O_3$ levels. However, the growth of the population and the number of cars in MC, the continuing usage of MTBE in reformulated gasoline, and the very high levels of volatile organic compounds have slowed and delayed the reduction of $O_3$ to acceptable levels. A serious problem in MC is the contribution of aromatic compounds to secondary organic aerosol formation through atmospheric transformation and the formation of oxidation products that are partially absorbed into organic films on pre-existing $PM_{2.5}$. Concentrations of $PM_{2.5}$ and $PM_{10}$ in MC are above the current annual standards. Lipopolysaccharides (LPS) detected in $PM_{10}$ samples show a range of 15.3 to 20.6 nanograms per milligram of $PM_{10}$, and PM samples from South Mexico City show the highest endotoxin concentrations at 59 EU/mg $PM_{10}$ (Bonner et al. 1998). Mexico City has significant sources of environmental endotoxins, including open-field waste areas, waste disposal dust, waste water treatment plants, open sewer channels, and daily outdoor deposits of 500 metric tons of animal and human fecal material.

### Control Cities

The control cities included Tlaxcala and Veracruz. Because of the combination of the relatively few contributing emission sources from industry and cars and the good ventilation conditions by the regional wind, criteria pollutants ($O_3$, $PM_{10}$, $SO_2$, $NO_2$, CO, and Pb) levels in control cities are below the current US standards. Three additional factors for the selection of the control cities included: (1) altitude above sea level similar to Mexico City (i.e., Tlaxcala); (2) dog necropsies from these cities have shown minimal pathology in lungs and hearts (Calderón-Garcidueñas et al. 2001); and (3) clinical studies in children in these cities have shown healthy children with no evidence of air-pollution–associated pathology (Calderón-Garcidueñas et al. 2003).

### Autopsy Selection

The study protocol was approved by the Institutional Review Boards for Human Studies at the institutions involved. We studied 47 subjects from 2 cohorts of clinically healthy, cognitively and neurologically intact children and adults, ages two to forty-five years, with an average age of 25.1 ± 1.5 y. The control cohort included subjects from low-polluted cities (n = 12) and the exposed cohort (n = 35) from MC. The forty-seven subjects had complete autopsies and neuropathological examinations and were included in the immunohistochemistry (IHC) and the real-time polymerase chain reaction (RT-PCR) studies. Data available for all subjects included age, gender, place of birth, place of residency, occupation, smoking habits, clinical histories, cause of death, and time between death and autopsy. Cause of death was considered for all subjects to rule out the possibility that infection, inflammatory events, drug exposure, brain ischemia, and hypoxia might impact the mRNA levels of the inflammatory markers measured in the study. Therefore, the selected cohorts had no clinical history or pathological evidence of short- or long-term inflammatory processes, administration of drugs, anti-inflammatory medications, hormones, or events such as cerebral ischemia or epilepsy.

### Necropsy and Tissue Preparation

Autopsies were performed 3.9 ± 1.1 hours after death. The postmortem period was similar for controls and pollution-exposed subjects. The skull was opened, and the OBs, trigeminal ganglia, and brain were removed. The right and left vagus nerves were exposed and dissected at the neck level, and a 10-cm section was cut along the OBs and selected areas from alternating right and left cerebral hemispheres, then quickly frozen and kept at –80°C. Frozen tissues for the RT-PCR were taken from the cortex and the white matter, taking care to make a perpendicular cut to the brain surface and keeping similar amounts of c

white matter for each method. In the midbrain section taken at the level of the superior colliculi, we dissected the substantia nigrae and the central grey stratum around the cerebral aqueduct. The right side was selected for the RT-PCR studies, and the left side was fixed in formaldehyde. Brain sections adjacent to the frozen material were immersed in 10% neutral formaldehyde, fixed for 48 hours, and transferred to 70% alcohol. Sections were taken from the OB, superior frontal gyrus, anteriomedial temporal lobe, hippocampus, basal ganglia, midbrain at the level of the superior colliculi, pons, medulla, neocerebellum, and trigeminal ganglia. Sections from lungs (upper-right lobe), peribronchial lymph nodes, heart (left and right ventricles), kidney, and liver were also taken. Paraffin sections 8 µm thick were cut and routinely stained with hematoxylin and eosin (H & E).

Immunohistochemistry (IHC) was performed on sections from the OB, frontal lobe, hippocampus, midbrain, pons, trigeminal ganglia, heart, and lungs. The sections were deparaffinized and immunostained as described previously (Calderón-Garcidueñas et al. 2004). Negative controls included omission or substitution of primary antibodies by nonspecific, isotype-matched antibodies. Positive and negative controls were included for each antibody. In double IHC, detection of β amyloid$_{1–42}$ was followed by GFAP staining, and CD163 was combined with glucose transporter type 1 (Glut-1). The brain histopathologic parameters evaluated included: vascular changes; the presence of histological elements characteristic of neuronal, glial necrosis, or apoptosis; and the distribution and characteristics of astrocytes. Sections were read blindly by one neuropathologist and one general pathologist with no access to the codes regarding the subjects' data. Electron microscopy was performed in frontal, trigeminal ganglia, and lungs of control and MC samples. Samples were fixed in 2% paraformaldehyde, 2% glutaraldehyde in sodium phosphate buffer (0.1M, pH 7.4), post-fixed in 1% osmium tetraoxide, and embedded in Epon. Semithin sections (0.5–1 µm) were cut and then stained with toluidine blue for light microscopy examination. Ultrathin sections (60–90 nm) were cut and collected on slot grids previously covered with formvar membrane. Sections were stained with uranyl acetate and lead citrate and examined with a Carl Zeiss EM109T (Germany) or a JEM-1011 (Japan). For immunofluorescence staining, prior to staining, 10- to 20-µm paraffin-embedded tissue sections were dewaxed, rehydrated, and pretreated by incubation with warm (37°C) trypsin 0.1% in phosphate-buffered saline (PBS) with $CaCl_2$ (PBS-$CaCl_2$) for ten minutes. Sections were then washed in PBS and incubated with the primary antibodies overnight at 4°C. After washing, incubation with secondary antibodies was done for four hours at room temperature. Primary antibodies were diluted as follows in PBS with 0.5% BSA: rabbit anti-

Glut-1, mouse CD163, VCAM-1, and ZO-1. Secondary antibody included goat antirabbit cyanine 5 and goat anti mouse Alexa fluor 488 and 568 at 1:100 (InVitrogen). Sections were mounted in PBS/glycerol (2:1) containing 170 mg/mL Mowiol 4–88 (Calbiochem, VWR International). For the confocal microscopy using the ZO-1 antibodies, we prepared smears of frontal fresh brain of seventeen cases, six controls, and eleven MC (APOE 3/3 and 4) subjects, fixed them in cold acetone for ten minutes, and air-dried the slides. Vessel diameters and tight juntion (TJ) abnormalities were assessed by two independent observers, and vessels were scored as normal or abnormal on the basis of the ZO-1 staining of their TJs. Selected areas with blood vessels were examined, and an average of one hundred vessels were visualized for the integrity of the ZO-1 staining. Fluorescence was examined using a BioRad Radiance 2000 laser scanning confocal on an inverted Nikon TE 300 microscope. Images were processed and visualized with LaserSharp software (version 2000, BioRad Microscience, Hertfordshire, UK).

Estimation of mRNA abundance was by real-time RT-PCR. Total RNA was extracted from frozen tissues including lungs, OB, frontal cortex, hippocampus, substantia nigrae, periaqueductal grey, and vagus nerves, using Trizol Reagent (Invitrogen Corp, Carlsbad, CA) according to the manufacturer's instructions. Random-primed first-strand cDNAs were generated as described (Calderón-Garcidueñas et al. 2004). Relative abundances of mRNAs encoding COX2, IL-1β, and CD14 were estimated by quantitative fluorogenic 5' nuclease (TaqMan) assay of the first-strand cDNAs as described (Calderón-Garcidueñas et al. 2004). Primers and fluorophore-labeled TaqMan probes targeting human COX2, IL-1β, and CD14 were designed using Primer Designer software (Scientific and Educational Software, Durham, NC) based on sequence information in GenBank.

For Asp299Gly and APOE genotyping, Asp299Gly genotype was determined using an allelic discrimination assay protocol according to Applied Biosystems (ABI). The aspartic-acid-to-glycine change at residue 299 results from the substitution of an adenosine to glycine at nucleotide 896 from the start codon of the TLR4 cDNA.The portion of the TLR4 gene containing the polymorphism was amplified using the PCR on the ABI Prism 7700 instrument. For the APOE genotyping, DNA was isolated from the frontal cortex as described and genotyped for the HhaI restriction site polymorphism in the APOE gene.

### Statistics

Statistics were performed using Stata statistical software (College Station, TX). We applied the parametric procedure that considers the differences among variances of the variables of

interest—COX2, IL-1β, and CD14 mRNA abundance in controls and exposed subjects. Significance was assumed at $p < .05$. Data are expressed as mean values ± SD.

## Results

### Air Quality Data

Residents in Mexico City have been chronically exposed to significant concentrations of $O_3$ and PM for the past two decades (Figure 1). The climatic conditions in Mexico City are relatively stable, thus pollutants concentrations are consistent year after year. Figure 1A illustrates the long-term trend (1986–2006) of the number of exceedances per year of the eight-hour $O_3$ air quality standard (0.085 ppm over any eight-hour period, not to be exceeded in three years) average concentrations as well as their 90th and 50th percentiles for eight-hour averages determined for the whole Mexico City Metropolitan Area (MCMA). The higher eight-hour average $O_3$ concentrations coincide with the times children and teens are outdoors during the school recess and physical education periods as well as when they play outdoors at home (Villarreal-Calderón et al. 2002). Figure 1B shows the trends of the number of days above the $PM_{10}$ (10 μm or less in aerodynamic diameter) twenty-four-hour average air quality standard (150 $\mu g/m^3$, not be exceeded more than once per year), the maximum of the daily $PM_{10}$ average concentrations, and the 50th percentile for 24-hour $PM_{10}$ concentration data registered in the whole MCMA from 1990 to 2006. Because of the existing high correlation between secondary organic aerosols and photochemical processes, $PM_{10}$ concentrations in Mexico City also tend to peak during the midafternoon hours, coinciding with children's activities (Villarreal-Calderón et al. 2002). Figure 1C illustrates $PM_{2.5}$ (2.5 μm or less in aerodynamic diameter) twenty-four-hour and annual concentrations for five different regions in MC for the years 2003–2006. Residents of MC are exposed to concentrations of $PM_{2.5}$ above the standards year after year. The air pollutant data from MC were obtained from the MC Ambient Air Monitoring Network.

### Study Population

The primary cause of death was accidents resulting in immediate death. The average age for the study cohorts of twelve controls and thirty-five highly exposed subjects was 26.4 ± 3.7 and 24.6 ± 1.6 years, respectively ($p = .66$) (Tables 1 and 2). The cohorts included thirteen children aged two to seventeen years (n = 4 in the control and n = 9 in the MC group), average age 13.2 ± 3.7 and 12.6 ± 1.7 respectively ($p = .33$), and within both cohorts there

were twenty-three subjects younger than twenty-five years (Table 1). The occupations in both cohorts included elementary, middle, and high school as well as college students and blue- and white-collar workers. Based on the careful evaluation of the medical information available and the results of the autopsy, each subject was considered to be clinically healthy and cognitively and neurologically intact prior to his or her demise.

### Real-time PCR mRNA Analysis of COX2, IL-1β, and CD14

Real-time, rapid-cycle PCR analysis of COX2, IL-1β, and CD14 in lungs, OB, frontal cortex, hippocampus, substantia nigrae, periaqueductal gray, and vagus nerves from 47 subjects indicated that the corresponding mRNA was present in each of the samples analyzed (Table 3). When samples were stratified according to the subject's residency (MC vs. low-polluted cities), there was a significant difference in mRNA for COX2 in lung ($p$ = 0.01), OB ($p$ = .0002), frontal cortex ($p$ = .008), substantia nigrae ($p$ = .03), left vagus (p = .03), and right vagus (p = .0002), whereas it was not significant for hippocampus ($p$ = .1) and periaqueductal gray ($p$ = .1) (Table 3). When MC subjects were graphed by age for OB mRNA COX2 values, there were five subjects (APOE ε 3/3) identified with the highest mRNA COX2 values; these subjects ranged in age between seven and thirty-four years, and four of them were teenagers. Three of these teens already exhibited Aβ42 in their OBs, and one of them also exhibited α-synuclein. The youngest child with the high OB COX2 value did not have Aβ42 or α-synuclein in his OBs. Age graphs for the substantia nigrae pars compacta SNC/COX2 dataset showed a cluster of four subjects with the highest mRNA COX2 values ranging in age from two to forty-five years; three of these subjects, including an eleven-year-old boy, had α-synuclein in OB and/or neurons in brain stem nuclei. When frontal mRNA COX2 samples were graphed by age, the higher values were seen in subjects in the third decade and older. The higher values of lung COX2 were seen in eight MC subjects aged two to forty-five years; these subjects, with the exception of a two-year-old boy, exhibited significant deposition of PM in interstitial spaces, alveolar macrophages, and subpleural regions. For the vagus nerves, the subjects with the higher COX2 values for the left were different—except for one twenty-year-old male APOE ε 3/4 subject—from the subjects with the higher COX2 right vagus values, and two of the higher COX2 vagus subjects also had the higher IL-1β values. The subject with the higher COX2 values for the left vagus, a thirty-four-year-old male APOE ε 3/3, exhibited α-synuclein in the dorsal nucleus of the vagus and in neuronal groups in the pons and medulla. For IL-1β, the frontal cortex ($p$ = .0002) and the OB ($p$ = .003) were significantly higher in MC subjects vs. controls, whereas it was not significant for lung, hippocampus, substantia nigrae, periaqueductal gray, and vagus nerves. The higher IL-1β mRNA values for both OB

frontal cortex corresponded to teens and young adults. Significant upregulation of CD14 was present in the OB ($p$ = .04), and the right ($p$ = .02) and left ($p$ = .01) vagus in MC subjects. The left vagus had the highest CD14 values across all subjects.

## Clinical and Gross Pathological Observations

### Non-CNS Findings

Tracheal epithelium showed patchy areas of squamous metaplasia and submucosal chronic inflammatory infiltrates in MC subjects over the age of twenty-five years. Nonperfused lungs from MC subjects displayed patchy clusters of alveolar macrophages filled with PM, bronchiolar smooth muscle cell hyperplasia, chronic mononuclear cell infiltrates, and macrophages filled with PM surrounding the bronchiolar walls and extending into adjacent vascular structures. In nine MC subjects there was extensive deposition of PM-laden macrophages in the subpleural regions along with mononuclear inflammatory infiltrates, smooth muscle cell hyperplasia of the pulmonary veins, and clusters of macrophages in the submucosa of the medium-sized bronchi. Peribronchial lymph nodes were grossly black in subjects over the age of twenty-five years and were loaded with PM (Figure 2A). Subjects from control cities exhibited small numbers of alveolar macrophages and rare foci of inflammatory cells in association with either terminal bronchioles or pulmonary blood vessels. Peribronchial lymph nodes showed small clusters of PM-containing macrophages. The higher lung values of mRNA COX2 were seen in eight of nine subjects, with the higher loads of PM in subpleural regions. Ganglion cells present in the bronchial walls, as well as Schwann cells in bronchial nerves, exhibit punctuate α-synuclein (Figures 2B and 2C). Nerve fibers in large bronchi also exhibit foci of mononuclear cells. Heart sections in MC residents showed clusters of perivascular partially degranulated mast cells, whereas nerve fibers on the epicardial surface exhibit positive α-synuclein punctuate pattern not seen in the control subjects. Liver sections from six MC residents showed PM in Kupffer cells (Figure 2D), and in macrophage-like cells in the portal spaces. These six subjects also had the most PM in their lungs. No liver abnormalities were seen in the control cohort.

### Lung Electron Microscopy

One-micrometer–thick toluidine blue sections from MC teenagers and young adults showed neutrophils attached to alveolar capillary endothelial cells (Figure 2E). The alveolar walls exhibited collagen interstitial fibers, and the endothelial cells exhibited numerous fronds surrounding red blood cells (RBC) (Figure 2F). The RBC exhibited aggregation of particles

along the cytoplasmic membrane and established discrete contacts with endothelial cell cytoplasmic vacuoles lined by particulate material (Figure 2G). Higher magnifications of RBC in lung capillaries revealed ultrafine PM (Figure 2H).

### CNS Gross Findings

Gross brain examination was unremarkable in all subjects.

### Brain Histopathology

For the olfactory nerve and bulb, four of the thirty-five MC subjects, including a fourteen-year-old boy, exhibited a significant amount of black PM in the cytoplasm of neuron-specific enolase (NSE)-positive cells at the glomerular region (Figure 3A). COX2 stained the cytoplasm of mitral and tufted neurons and olfactory ensheathing cells. Aβ42 was seen in ensheathing cells, astrocytes in the olfactory nerve, and in OB neurons in six of eighteen MC APOE ε 3/3 subjects younger than twenty-five years (Table 2), the youngest an eleven-year-old boy (Figure 3B). Corporae amylacea were numerous along the length of the olfactory nerves starting in the late teens. Reactive gliosis (GFAP-positive astrocytes) was present in all layers of the OB in all exposed subjects (including external and internal plexiform, mitral cell layers, and the olfactory glomeruli). Alpha-synuclein was present in the form of Lewy neurites, as well as granular punctuate cytoplasmic deposits in NSE-positive cells in the glomerular, mitral, and granular cell layers in four of eighteen MC subjects younger than twenty-five years old (Table 1, Figure 3C); the youngest was an eleven-year-old boy (Figure 3D). In the trigeminal ganglia and nerves, partially degranulated mast cells were seen in close proximity to the ganglion cells (Figure 3E). Perineurial blood vessels exhibited vacuolated endothelial cells and marginal WBCs.

### Cortical Sections

As to vascular changes, teens exhibited significant amounts of lipofuscin in endothelial cortical capillaries cells. Perivascular hemosiderin-laden macrophages were seen around small venules and arterioles in both gray and white matter, the latter being foremost; these changes were already prominent in the eleven-year-old MC boy in this series. Intact RBCs inside macrophages were identified alongside the hemosiderin-laden macrophages (Figure 3F). In five MC subjects, cortical blood vessels exhibit platelet thrombi (Figure 3G). Exposed subjects exhibited positive prothrombin (PT) staining outside blood vessel walls, predominantly in the white matter (Figure 3 H). Perivascular macrophages as well as reactive astrocytes were positive for prothrombin in the proximity of blood vessels with PT

the walls. No PT outside of blood vessels was seen in the controls. Clusters of mononuclear cells around blood vessels in the frontal and temporal cortex, subicular area, and the brain stem were a frequent finding in MC subjects regardless of age (Figure 4A). These mononuclear cells were positive for CD68, CD163, and HLA-DR. CD163-positive cells were present predominantly in perivascular locations in the cortex and to a lesser degree in the neuropil as activated positive microglia (Figure 4B). CD68 stained numerous white matter microglia-like cells in highly exposed individuals. Positive CD68 and HLA-DR cells were seen predominantly in the white matter (Figures 4C and 4D), and positive perivascular cells were seen in the cortex in MC subjects as young as two years of age. In MC subjects, numerous partially degranulated mast cells exhibit positive tryptase granules (Figure 4E), particulary in the white matter, whereas frontal neurons exhibited positive staining in their cytoplasm. In controls, however, only occasional tryptase positive perivascular cells were seen, and the neurons were negative. VCAM-1 strongly stained cortical endothelial cells in MC subjects (Figure 4F), whereas ICAM-1 was positive for astrocytes and microglia cells in both the cortex and the white matter. Nitrotyrosine (NT) positive cells were present in all exposed individuals. NT immunorectivity was present as diffuse cytoplasm neuronal staining in frontal neurons as well as inclusions in glial cells, including astrocytes and microglia. Abundant NT-positive, macrophage-like cells were seen in perivascular white matter locations (Figure 4G), as well in endothelial cells. Control subjects exhibited an occasional perivascular positive cell. NFκB was positive in the nuclei of endothelial cells in cortical capillaries (Figure 4H) and perivascular macrophages in MC residents. NFκB nuclear positivity was not seen in control subjects. iNOS-positive cells included astrocytes and neurons in cortical regions and the OB of MC residents. COX2 immunoreactivity was seen in neuronal cell bodies and dendrites, as well as endothelial cells of small capillaries and arterioles in the frontal cortex. Exposed subjects exhibited strong endothelial COX2 staining in both cortex and white matter. In control subjects, the staining was confined to neurons. 8-0HdG positivity was present predominantly in pyramidal frontal cells and, to a lesser degree, in astrocytes in the white matter of MC subjects. Astrocytes with a small amount of cytoplasm were seen around blood vessels and neurons in the frontal cortex; a few of these astrocytes were positive for GFAP. Patchy cortical GFAP-positive astrocytes were prominent in MC children (present in the youngest, two years old) and teens. GFAP-positive astrocytes increased in the cortex with age. Reactive astrocytes were focally prominent in subpial areas and perivascular deep white matter of all exposed individuals. Immunoreactivity for Aβ42 was seen in the cytoplasm of neurons in the frontal and temporal cortices, in the smooth muscle cells of cortical vessels, and in both diffuse and mature senile plaques. In MC residents, Aβ42 selectively

accumulated in the perikaryon of pyramidal frontal neurons as discrete granules and was present in cortical and white matter astrocytes and in sub-arachnoid and cortical blood vessels. Neuronal Aβ42 was identified in APOE ε 3/3 children as young as eleven years old, whereas diffuse plaques were first seen in seventeen-year-olds (Figure 5A). Mature Aβ42 plaques were abundant in subjects in the fourth decade (Figure 5B). In the cohort of APOE ε 3/3 MC subjects under twenty-five years of age, nine of seventeen exhibited Aβ42 positivity in the frontal cortex (Table 1). In sharp contrast, in the cohort of APOE ε 4 MC subjects (Table 4), the four youngest subjects (ages fifteen, twenty, twenty-two, and twenty-five) all exhibited Aβ42 in the OB, blood vessels, cortical neurons, and/or in diffuse plaques. There were three controls who were heterozygous for APOE 4 (ages thirty-six, forty-four, and forty-five), and two of these subjects had Aβ42 immunoreactivity. None of the forty-seven subjects fulfilled morphological Alzheimer's criteria as described in the Consortium to Establish a Registry for Alzheimer's Disease (CERAD), Braak stages, and NIA-Reagan Institute criteria (Lilian Calderón-Garcidueñas, unpublished data).

### Confocal Microscopy for Tight Junctional Abnormalities Zonula Occludens Ab (ZO-1)

The majority of examined vessels were < 100 μm in diameter. In the control group APOE β 3/3 (n = 4, age = 16 ± 4.88 years), there were 3.8 ± 1.08% of vessels with abnormal ZO-1 TJs. Mexico City subjects APOE β 3/3 (n = 8, age 13.25 ± 2.36 years) exhibited 30.8 ± 5.9%, whereas APOE β 4/4 and 3/4 (n = 5, including 2 controls) had 62.2 ± 7.36% of the vessels with discontinuous or punctuate staining in the frontal cortex (Figure 5C). There was a significant difference in the number of abnormal tight junctions between APOE β 3/3 controls and MC subjects ($p$ = .01) and vs APOE β 3/4 ($p$ = .0002), whereas there was also a significant difference between MC APOE β 3/3 vs. 3/4 ($p$ = .007).

Brainstem: vascular changes in the brainstem, including the midbrain, were similar to the ones described for the neocor-tex. Exposed subjects exhibit significant VCAM-1 staining of endothelial cells in capillaries and small venous and arteriolar vessels in the midbrain. CD163 and HLA-DR strongly stained mononuclear perivascular cells, whereas CD68 stained microglia-like cells in the substantia nigrae pars compacta (SNC) region, superior colliculus, red nucleus, tegmental tract, and medial lemniscus. A few tryptase-stained perivascular cells were seen in some of the exposed subjects. There was a significant degranulation of SNC in subjects in their twenties and early thirties. The degranulation was accompanied by numerous macrophages loaded with melanin pigment around the degranulated neurons and in perivascular locations. These changes were also seen in the Asp299Gly TLR4

polymorphism subjects. The MC woman APOE ε 4/4 exhibited α-synuclein positivity in substantia nigrae neurons and mesencephalic V neurons and displayed significant degranulation of SNC pigmented cells with numerous melanin-laden macrophages. In MC residents, NT and 8-0HdG positivity were present in raphe neurons, mesencephalic V neurons, and glial cells in the medial raphe (Figure 5E). 8-0HdG-positive neurons were also seen in the trigeminal thalamic ventral tract. Alpha-synuclein granular cytoplasmic neuronal staining involved neurons in the trigeminal thalamic tract, mesencephalic V, reticular and raphe nuclei, the glossopharyngeal-vagus complexes, and the SNC (Figure 5F) in exposed subjects as young as seventeen years of age (Table 1). Perivascular macrophages with hemosiderin pigment and intact RBC were seen in capillaries throughout the brain stem, including the ones in the regions of cranial nerve nuclei (i.e., mesencephalic trigeminal neurons). Fibrin thrombi were seen at all levels of the brain stem in small blood vessels in exposed subjects.

### Evaluation of APOE ε 3/4 and 4/4 Subjects

All MC APOE ε 4 either heterozygous or homozygous subjects had Aβ42 in neurons and blood vessels in the frontal cortex and the hippocampus, including the twenty-year-old male with a mutant TLR4 genotype (Table 4). Vascular changes, cortical reactive GFAP-positive astrocytes and white matter gliosis were more prominent than in the APOE ε 3/3 age-matched MC cohort. The only APOE ε 4/4 subject, a thirty-two-year-old MC woman, had scattered foci of perivascular monuclear cells in the hippocampi, as well as platelet thrombi in small blood vessels. This woman had Aβ42 in her OBs, cortical neurons, and cortical and subarach-noid blood vessels, in addition to α-synuclein immunoreactivity in the substantia nigrae and neurons from the mesencephalic trigeminal nerve. Subjects with the APOE ε 4 allele displayed ZO-1 discontinuous or punctuate staining in 62.2% of their vessels throughout the frontal cortex, in sharp contrast to the 30.8% in APOE ε 3/3 subjects ($p$ = .007). Assessment of accumulation of Aβ42 and α-synuclein as a function of age and residency (Tables 5 and 6) showed that 58.8% of APOE ε 2/3, 3/3 subjects under the age of twenty-five who were residents of MC exhibit Aβ42 accumulation (average age 17.4 years), whereas in the same group 23.5% already had α-synuclein detectable by IHC. Accumulation of both Aβ42 and α-synuclein starts in the teen years in MC residents (Tables 5 and 6).

### Electron Microscopy

Frontal capillaries exhibited RBC with ultrafine particles in their cytoplasm, along with aggregation of intramembrane UFPM and establishment of discrete contacts with

endothelial cell cytoplasmic membranes (Figure 5G). Mononuclear cells established a close contact with the capillary outside the BBB, and UFPM was seen frequently at the interphase. Trigeminal ganglia capillary sections also revealed the presence of discrete contacts between the RBC and the endothelial cells and increased caveoli (Figure 5H with insert).

## Discussion

Clinically healthy, cognitively and neurologically intact children, teenagers, and young adults with a lifetime exposure to significant concentrations of air pollutants including $O_3$, PM, and PM-LPS exhibit an upregulation of mRNA COX2, IL-1β, and a key innate immunity receptor CD14 in the OB, frontal cortex, substantia nigrae, and/or vagus nerves, as well as early disruption of the tight junctions in frontal blood vessels. These subjects exhibit nuclear NFκB in brain endothelial cells as well as evidence of an activated inflamed cerebral endothelium, with an altered BBB and trafficking of inflammatory cells in perivascular areas and in the neuropil. The OB mRNA COX2 upregulation, the frontal disruption of the BBB, and the endothelial nuclear NFκB are early key findings in the highly exposed cohort. Inflammatory cell trafficking and Aβ42 accumulation in the OB and frontal cortex are seen in prepuberal children with no known risk factors for Alzheimer's disease. Alpha-synuclein Lewy neurites and punctuate α-synuclein neuronal accumulation are seen in the OB in children as young as eleven years of age, and in teens and young adults the α-synuclein immunoreactivity was also identified in the dorsal nucleus of the vagus, mesencephalic V, trigeminal thalamic tract, substantia nigrae, and in lung and heart autonomic ganglia and nerves.

The presence of PM in olfactory bulb neurons, in luminal erythrocytes from capillaries in lung, frontal and trigeminal ganglia, and in Kupffer cells, along with the translocation of UFPM from RBC to endothelial cells in capillary lungs, and from RBC to endothelial cells and to perivascular macrophage-like cells in frontal capillaries are very important observations in these highly exposed individuals. The fact that PM is directly reaching the brain parenchyma, along with the early disruption of the BBB and the vagal upregulation of CD14 capable of activating inflammatory processes in the brain stem, are key findings that need to be analyzed in terms of their potential impact on neuroinflammation and neurodegeneration.

There has been a growing interest in the identification of fine and ultrafine PM in urban air and their health effects (Donaldson 2003; Oberdorster et al. 2002), as well as how these particles reach the brain (Dorman et al. 2002; Henriksson et al. 1997). Moreover, neurodegenerative effects have been reported in experimental animals using UFPM (Block et

al. 2004; Peters et al. 2006), and in dogs and human beings exposed to urban environments (Calderón-Garcidueñas et al. 2002; Calderón-Garcidueñas, Maronpot et al. 2003; Peters et al. 2006). Fine and ultrafine PM exhibit biological activities that are detrimental to cells, including induction of oxidative stress with the consequent depletion of cell antioxidants, direct cytoxicity including mitochondrial dysfunction and altered phagocytic function, alteration of cell signaling pathways, and DNA and lipid damage (Donaldson 2003). Portals of entry of PM are of utmost importance in highly exposed subjects in MC, particularly children, since we have documented breakdown of the nasal barrier with significant accumulation of PM in and around nasal epithelial cells (Calderón-Garcidueñas et al. 2001; Calderón-Garcidueñas, Franco-Lira et al. 2007) and the transport of metals associated with PM to OB neurons (Calderón-Garcidueñas, Maronpot et al. 2003). Factors such as age, gender, weight, race, nostril shape, exercise level, minute ventilation, and outdoor time all contribute to the particle deposition and to lesser or higher risk from inhalation of pollutant PM in ambient air (Bennett et al. 2005; Villarreal-Calderón et al. 2002).

Early disruption of the BBB and translocation of UFPM likely contribute to damage of the BBB. An intact BBB is necessary for the proper functioning of the CNS by actively controlling cellular and molecular trafficking between the systemic circulation and the brain parenchyma (Abbott 2005). Brain capillaries represent the largest surface area blood–CNS interface where tight intercellular junctions constitute the morphological basis of the BBB (Lossinsky et al. 2004). The issue of a damaged BBB is important, since this barrier has the ability to respond to LPS, IL-1β, TNFα, and IL-6 (Nadeau and Rivest 1999; Rivest 2001). LPS and IL-1β upregulate adhesion molecules, increase leukocyte migration across the CNS endothelial cells, and regulate BBB permeability (Hickey 2001; Rothwell and Luheshi 2000), whereas TNFα and IL-6 disrupt the BBB through the release of endothelial nitric oxide or, in the case of a transgenic animal overexpressing IL-6, the lack of BBB development (Brett et al. 1995; Farkas et al. 2006). Clinically healthy children in MC have evidence of systemic inflammation with increased sustained levels of prostaglandin E metabolite, IL-6, IL-1β, and a systemic response to their LPS-PM exposure through upregulation of mCD14 and two transporting LPS proteins: lactoferrin and heat shock protein 60 (Calderón-Garcidueñas Mora Tiscareño et al. 2003; Calderón-Garcidueñas, Franco-Lira et al. 2007; Calderón-Garcidueñas, Vincent et al. 2007). Since brain blood vessels express receptors for TNFα, IL-1β, and IL-6 (Nadeau and Rivest 1999), and TNFα and IL-1β can evoke expression of inflammatory mediator genes, such as COX2 (Rivest 2001) within the brain capillary endothelium, our findings of an early BBB disruption and CD14 upregulation suggest that systemic cytokines

could be key early CNS vascular aggressors. Moreover, circulating cytokines can gain access to the brain by being transported across the BBB (Nguyen et al. 2002; Rivest 2001; Pan and Kastin 2001) and are able to evoke additional inflammatory mediator expression by vascular-associated microglia (Griffin et al. 2002), further increasing the permeability of the BBB (Blamire et al. 2000). Systemic and local brain production of cytokines are implicated in contributing to the initiation, propagation, and regulation of immune and inflammatory circuits (Benveniste 1998; Cunningham et al. 2005). IL-1β is the most important molecule capable of modulating cerebral functions during systemic and localized inflammation (Ferrari et al. 2006; Griffin et al. 2002; Rothwell and Luheshi 2000). Zhang and Rivest proposed that circulating LPS and cytokines could bind to their cognate receptors onto endothelial and/or monocytic cells lining the BBB, which in turn will lead to proinflammatory signaling and transcription of the receptors for different proinflammatory ligands that can stimulate NFκB kinases and mitogen-activated protein (MAP) and the enzymes responsible for PGE2 formation in the cerebral tissue (Zhang et al. 2003). Zhang and Rivest proposed responses to systemic immune stimuli likely apply to our chronically air-pollution–exposed subjects.

A critical finding is the endothelial nuclear NFκB activation present in the brain capillaries of young exposed subjects. NFκB activation depends on varied stimuli such as cytokines, LPS, and DNA damage (Pahl 1999); activation is tightly regulated and quickly shortened through feedback inhibition following the initial activating stimulus (Xiao et al. 2006). However, persistant activation (i.e., continuous exposure to significant levels of cytokines, UFPM, and/or PMLPS) results in deleterious effects.

Once the BBB is disrupted, significant leaking of RBC and proteins such as prothrombin may follow. There is an increment in the number of perivascular macrophages and microglia that expresses CD163, a scavenger receptor mediating the removal of hemoglobin-heptaglobin complexes, that is increased in inflammatory disorders (Kim et al. 2006). CD163 perivascular macrophages were common in the deep frontal and temporal white matter of MC subjects. Concomitantly with the increment in CD163, immunoreactivity for CD68 and HLA-DR in microglia, perivascular macrophages and endothelial cells were observed, in keeping with the inflammatory response. Intact and degranulated mast cells identified by means of tryptase monoclonal antibodies were seen in perivascular locations in frontal and temporal cortices, as well in trigeminal ganglia, and in peripheral autonomic nerves innervating the lungs and hearts in MC subjects, whereas in the control subjects mast cells were very rare and intact. Mast cells in the brain are normally observed in small numbers around the third ventricle, thalamus, hypothalamus, and meninges, and in the peripheral nervous s

association with inflammatory processes (Dropp 1979; Theoharides 1990). Mediators released by activated mast cells contribute to local inflammatory responses, regulating BBB permeability and angiogenesis and playing an active role in neuroinflammation (Ibrahim et al. 1996). More importantly, their presence in the context of the disruption of the BBB relates to their arrival in the CNS and PNS via the bloodstream following the trafficking of other inflammatory cells (Ibrahim et al. 1996). The identification of prothrombin in extravascular spaces and perivascular macrophages is a crucial finding in keeping with the BBB disruption (Mhatre et al. 2006), and it could be a contributing factor in the increased apolipoprotein immunoreactivity observed in MC dogs (Calderón-Garcidueñas et al. 2002), and as described by Mhatre et al. in a rat model of intraventricular infusion of prothrombin (Mhatre et al. 2006). The seminal work of Grammas et al. has shown that neurotoxic thrombin and inflammatory proteins are elevated in AD microvessels, a finding that is very relevant to our work. Rupture of the vascular basement membrane and leakage of prothrombin are described in the prefrontal cortex of Alzheimer's patients (Zipser et al. 2007).

Perivascular mononuclear cells are active and efficient antigen-presenting cells (Lossinsky et al. 2004). In a healthy brain the endothelial cells express very low levels of adhesion molecules required for leukocyte emigration (Lossinsky et al. 2004), a central pathogenic event in CNS inflammation (Hickey 2001). Leukocyte adhesion to endothelial cells is a crucial step to facilitate selective and effective capture of leukocytes (Hickey 2001), and for leukocytes to cross the BBB, they must first roll along the luminal endothelial cell (EC) surfaces to establish the initial cell–cell communication (Abbott 2005; Hickey 2001; Lossinky et al. 2004). In in vitro adhesion assays, binding of lymphocytes to inflamed brain vessels is mainly mediated by leukocyte function-associated antigen-1 and intracellular adhesion molecule-1, the late-activation antigen-4, and the vascular cell adhesion molecule-1 (Hickey 2001). EC activation is seen after the injection of TNFα and LPS (Nadeau and Rivest 1999; Pan and Kastin 2001; Rivest 2001), the latter of which represents an important component of PM in MC. In MC subjects including children, the luminal EC exhibit strong immunoreactivity for adhesion molecules such as VCAM-1 and ICAM-1 both in supra- and infratentorial regions. In keeping with the EC activation, two critical observations were described in this human study: the presence of UFPM in RBCs and the aggregation of intramembrane particles with the formation of patterned discrete contact points between endothelial cells and RBCs in the CNS, trigeminal ganglia, and lung capillaries of highly exposed people. The establishment of contact points between ECs and RBCs could represent a pathway for the exchange of PM between the activated endothelial cell and the UFPM-loaded RBCs, in keeping with the

capacity of ultrafine PM to penetrate RBC, as elegantly shown by Geiser and Rothen-Rutishauser (Geiser et al. 2005; Rothen-Rutishauser et al. 2006). Ultrafine particles are not membrane bound, which allows for direct access to intracellular proteins, organelles, and DNA, enhancing their toxic potential (Geiser et al. 2005). Further, the passage of PM to the brain following the RBC-activated EC is likely to be increased in subjects exposed to pollutants owing to the disruption of the BBB as described in previous lines, and it is likely related to the production of NO (Calderón-Garcidueñas et al. 2002; Thiel and Audus 2001). Plasmodium infected RBCs induce endothelial upregulation of ICAM-1 and give rise to endothelial cell microvilli or cytoplasmic fronds that touch the infected RBCs (Tripathi et al. 2006). The formation of endothelial fronds surrounding the RBC in the malaria-infected model is remarkably similar to our findings in the lung and trigeminal ganglia capillaries. Of utmost importance, the endothelial fronds/microvilli in the malaria model interfered with blood flow even after lysis of the infected RBCs (Tripathi et al. 2006), an indication that in our subjects the endothelial frond formation could account for a decreased blood flow in the involved areas.

Breakdown of the nasal barrier in pollution-exposed subjects may also contribute to brain inflammation by increasing the access of PM to the brain through the olfactory and trigeminal pathways. The finding of PM in the glomerular region of the OBs of MC residents indicates that particles are readily transported from the nasal cavity to the brain via the olfactory nerve, a pathway very well known in experimental animals exposed to metals (Dorman et al. 2002; Henriksson et al. 1997). Moreover, there is an early and significant upregulation of COX2, IL-1β, and CD14 in the OB, which is indicative of an ongoing inflammatory process. Further, the accumulation of Aβ42 and α-synuclein in the OB is associated with significant upregulation of mRNA COX2, whereas the presence of α-synuclein in the brain stem is related to COX2 upregulation in the substantia nigrae. The upregulation of COX2 is particularly relevant in these subjects already exhibiting Aβ42 accumulation, since COX2 potentiates β-amyloid peptide generation through alterations in γ secretase activity and apoptotic cell death and is indeed associated with the accumulation of Aβ42 (Qin et al. 2003; Xiang et al. 2002) and α-synuclein (Jellinger 2003). Both Aβ42 and α-synuclein are proteins capable of aggregation and misfolding, leading to progressive neurodegeneration that develops insidiously over the lifetime of the individual (Jellinger 2003; McGeer et al. 2006; Nguyen et al. 2002; Selkoe 2001, 2002). Given that axons from the olfactory sensory neurons project to the OB, and the primary axons of the projection neurons send off collateral branches to the olfactory nuclei, piriform cortex, entorhinal cortex, and amygdaloid

nuclei, and then to the hippocampal formation and the parahippocampal gyrus, it is expected that significant inflammatory process in the OB in these highly exposed subjects may translate into olfactory dysfunction, which is indeed the case in young adults (L. Calderón-Garcidueñas and M. Franco-Lira, pers. comm. 2007). Olfactory dysfunction is an early clinical finding in several neurodegenerative disorders, including Alzheimer and Parkinson's diseases (Hawkes 2003).

We have shown that the OB and the substantia nigrae are early targets of air pollution in young people, since the greater upregulation of mRNA COX2 was documented in teens and young adults. Alpha-synuclein accumulated as Lewy neurites and/or punctuate deposits in the OB, trigeminal thalamic tract, mesencephalic V, reticular and raphe nuclei, the glossopharyngeal-vagus complexes, and lung and heart autonomic ganglia in subjects as young as eleven years of age for the OB and the lung ganglion cells, and seventeen years for the brain stem findings. The brain stem findings in teens and young adults bring up three crucial issues: (1) the role the vagus nerves play in the brain stem inflammation development; (2) the accumulation of α-synuclein in target areas as a risk factor for the development of Parkinson's disease in exposed populations; and (3) the accumulation of α-synuclein as a neuroprotective or neurotoxic effect. We know that systemic cytokines could affect the CNS via sensory nerves such as the vagus. This could be a consequence of exposure to air pollutants, because IL-1β is recognized by chemosensory receptors located in vagal paraganglia in the vagus nerve at several levels, including the cervical, thoracic, and abdominal regions (Elmquist et al. 1997). Activation of the peripheral immune system drives viscerosensory pathways originating in the brain stem nucleus of the solitary tract and ventrolateral medulla in response to cytokine signaling in the vagus nerve (Elmquist et al. 1997). The vagus and glosopharyngeal nerves, with their chemosensitive afferent fibers, are major neural pathways that establish communication between the immune system and the brain, generating responses to proinflammatory mediators (Elmquist et al. 1997). Moreover, indirect activation of the vagus nerve can be accomplished by paraganglia activation (Goehler et al. 1999). Paraganglia are located in the thorax and abdomen and are positioned to sense immune products released in lymph nodes and visceral organs, and they express binding receptors for IL-1β (Goehler et al. 1999). Indeed, the vagus nerves play a role in the lung inflammation caused by diesel-soot rodent exposures (McQueen et al. 2007), further emphasizing their potential to extend the inflammatory response into the brain stem. The upregulation of COX2 in the vagus nerves was an expected finding, given the extensive innervation coverage of the vagus nerves in target organs exposed to PM and endotoxins

(i.e., lung, heart, and liver) (Kukanova and Mravec 2006; Uyama et al. 2004). Moreover, the presence of PM in Kupffer cells—the liver-resident macrophages (Uyama et al. 2004; Wake et al. 1989) responsible for the clearance of foreign material arriving from the circulation and the gut (Wake et al. 1989)—is a very interesting finding, given that the liver and the digestive tract are preferred sites for extrapulmonary translocation of ultrafine particles in human beings and rats (Oberdorster et al. 2002). Thus, the mRNA COX2 right vagus nerve's significant upregulation when compared to the left in MC residents could be an indication of the role the liver plays in the detoxification and clearance of foreign and altered-self substances including PM and LPS-PM in the parenchyma (Nolan 1975). The issue is important from the clinical point of view, since in Parkinson's disease there is substantial asymmetry of symptoms from the onset, with a marked preference for the right side (Djaldetti et al. 2006). Thus, the asymmetry could be explained for the PM factor, by the type and size of particles people are exposed to, and their fate in the lung and extrarespiratory anatomical areas (Daigle et al. 2003). Thus, in MC residents with a disrupted and ineffective nasal barrier, major concentrations of PM would be swallowed and thus enter the digestive system, the liver pathway, and the right vagus. Interestingly, whereas the substantia nigrae in the highly exposed subjects exhibited an upregulation of COX2 ($p$ = .03), IL-1β did not reach significance ($p$ = .06). In contrast, the periventricular grey adjacent to the SNC but not involved in the same neural pathways did not show upregulation of any of the selected inflammatory genes. Based on these findings we concluded that in subjects exposed to air pollution, the brain stem is taking part in the inflammatory process, either through local pathways or systemic inflammation or both, and the brain stem participation likely also depends on the PM entry pathways (i.e., digestive and lower respiratory systems).

Alpha-synuclein—an abundant brain 140 residue protein—is the culprit in Parkinson's disease (PD) (Braak et al. 2003; Eriksen et al. 2003; Fink 2006; Jellinger 2003). Synucleins are developmentally expressed, and α-synuclein is present in presynaptic terminals and in both soluble and membrane-associated brain fractions (Fink 2006; Eriksen et al. 2003; Jellinger 2003). Substantial evidence suggests that α-synuclein aggregation is a critical step in PD and other synucleopathies (Fink 2006; Jellinger 2003), and a pathway going from normal soluble to abnormal misfolded filamentous proteins is a key process regardless of the primary disorder (Fink 2006; Jellinger 2003). Factors affecting the kinetics of α-synuclein fibrillation include oxidative stress, pesticides, metals, glycosaminoglycans, lipids, and macromolecular crowding (Fink 2006). Linse et al. demonstrated that nanoparticles enhance the rate of protein fibrillation by decreasing the lag time for nucleation, a novel mechanism that could

be applicable to both Aβ42 and α-synuclein in the scenario of air pollution. Oxidative stress is present in the brain stem of these MC subjects, as evidenced by the presence of cells positive for 8-OHdG and NT and the upregulation of COX2 in the substantia nigrae, which could result in the production of ROS (Choi et al. 2006; Minghetti 2005). Early and sustained production of COX2 results in the production of free radicals in the process of converting arachidonic acid to precursors of vasoactive prostaglandins (Choi et al. 2006; Minghetti 2005). The presence of aggregated α-synuclein in target CNS and PNS regions in these high-air-pollution–exposed young cohorts follows the characteristic topographical distribution of early PD lesions, as described by Braak and colleagues (Braak et al. 2003, 2006; Del Tredeci et al. 2002), that is, OB, lower brain stem, and ganglionic autonomic cells. These prepuberal teens and young adults can be identified by their aggregated α-synuclein as being in Braak stages 1 and 2, the presymptomatic PD stage. Recent observations among MC pediatric cardiologists of an increased number of otherwise healthy children with syncope could offer evidence of heart autonomic and lower brain stem involvement as we have shown here (Dr. Alfredo Bobadilla-Aguirre, pers. comm., November 14, 2006). We strongly suggest that the Braak et al. proposal (2003) about a "putative environmental pathogen capable of passing the gastric epithelial lining might induce α-synuclein misfolding and aggregation" could indeed be related to PM gaining access to the brain through the respiratory and gastrointestinal vagus pathway in subjects exposed to significant PM concentrations for long periods of time. A controversial issue has to be addressed in this scenario: is the aggregation of α-synuclein neuroprotective or toxic in these young subjects? (Quilty et al. 2006; Sidhu et al. 2004) It appears that in tissue culture and with relatively low levels of oxidative stress, increased α-synuclein offers neuroprotection (Quilty et al. 2006), and it is also clear that the level of expression is crucial to confer either protection or toxicity (Sidhu et al. 2004). Given that the potential factors (oxidative stress, COX2 upregulation, vascular inflammation, nanoparticles) likely accounting for the aggregation of α-synuclein in these air-pollution–exposed subjects are both intense and prolonged, we favor the idea that α-synuclein acquires neurotoxic properties in these cohorts.

Chronic oxidative stress is a major contributing factor in the pathogenesis of both Alzheimer's and Parkinson's diseases (Nunomura et al. 2006; Quilty et al. 2006). We previously described significant oxidative DNA damage (genomic DNA apurinic/apyrimidinic sites) in both MC dogs and human beings in the OB and the frontal cortex (Calderón-Garcidueñas et al. 2002; Calderón-Garcidueñas, Maronpot et al. 2003). Our human data support previous work from Nunomura et al., Forero et al., and Zhu et al. stating that

oxidative stress is early and precedes neuropathological manifestations of AD. We could add that brain oxidative stress starts in childhood and the teen years and is accompanied by accumulation of both Aβ42 and α-synuclein in the scenario of air pollution exposure.

Apolipoprotein E is the susceptibility gene with the clearest link to late-onset Alzheimer's disease, although the ε 4 genotype alone is insufficient to predict an individual's risk for AD (Wishart et al. 2006). In this work we have shown that carriers of an ε 4 allele residing in MC accelerate their Aβ42 accumulation by one decade compared to 3/3 carriers (Table 5). On the other hand, there is Aβ42 brain immunoreactivity in 58.8% of young MC residents (17.41 ± 1.5 years) with ε 3 alleles, and 80% in the older cohort (>25 years [35.2 ± 1.9 years]). These results suggest that cumulative exposures and age are key factors. It is interesting to point to this observation, because the deposits of Aβ42 start in childhood and the teen years in MC residents, and we know that these subjects do not fulfill current morphological AD criteria, thus these younger years constitute a time frame that is important in terms of pharmacological protection of our exposed populations. Alpha-synuclein accumulation also starts in the teens in highly exposed subjects, moreover, as expected we found no differences in APOE 4 carriers (Table 6).

Given that all ε 4 MC subjects—including the fifteen-year-old boy—had accumulation of Aβ42 obligates us to entertain the possibility that in the context of exposure to severe air pollution, the presence of an ε 4 accelerates the AD-like pathology. Since regional brain atrophy in the right medial temporal and bilateral frontotemporal regions (Wishart et al. 2006) and altered fractional anisotrophy (Persson et al. 2006)—a marker of white matter integrity—have been described in cognitively intact adults with homozygous or heterozygous ε 4 status, it is possible than MC APOE ε 4 teens already display similar alterations, a major issue because maturation of white-matter pathways is crucial in cognitive, behavioral, emotional, and motor development during childhood and the teen years.

There is no doubt that some subjects in this highly exposed MC cohort responded mainly with supratentorial pathology, deposition of Aβ42, and formation of diffuse amyloid plaques, whereas for others the response was mainly infratentorial, with the substantia nigrae and the vagus upregulation of COX2 and the deposition of α-synuclein in brain stem nuclei. A small group of subjects displayed both supra- and infratentorial pathology. This pattern of findings pointing toward Alzheimer's and/or Parkinson's-like pathology resembles the distribution of AD/PD patients with overlaps (Kurosinski et al. 2002). Given the common denominators between these two major neurode-generative diseases, our findings are expected.

The age issue of detection of Aβ42 in teens is important, given that higher mRNA IL-1β expression is seen in frontal cortex in teens and young adults under the age of twenty-five, whereas the higher values for mRNA COX2 were seen in adults over the age of thirty. Thus, teens' frontal cortices exhibit early IL-1β upregulation. Cytokines play a central role in the self-propagation of neuroinflammation, with IL-1β having a prominent function (Minghetti 2005). The early upregulation of IL-1β in the frontal lobe of young subjects is of utmost importance, because this proinflammatory cytokine has been associated with BBB disruption; recruitment of inflammatory cells into the CNS (Ferrari et al. 2006); sustained upregulation of IL-8, VCAM-1, and ICAM-1 in astrocytes (Moynagh 2005); and with neuronal, glial, and endothelial injury through strong activation of the classical IL-1 signaling pathway, activation of MAPKs and NFκB (reviewed in Allan et al. 2005). Equally crucial is the role of IL-1β in the transformation of diffuse Aβ in mature plaques (Akiyama et al. 2000). NFκB is a crucial mediator in the IL-1β signal, and NFκB activation is sustained in astrocytes in response to IL-1 stimulation (Moynagh 2005).

The upregulation of CD14 may significantly contribute to the neuroinflammatory response in air-pollution–exposed subjects, particularly those exposed to significant amounts of PM-associated LPS, hence the upregulation of mRNA CD14 in the OBs and vagal nerves could indicate a brisk response of the innate immune system to LPS. Interestingly, although mCOX2 was significantly upregulated in the right vagus ($p$ =.0002) versus the left ($p$ = .03), CD14 expression was less, presumably reflecting the liver capacity to inactivate LPS. Fassbender et al. showed that CD14 binds Aβ and mediates Aβ-induced microglial and monocytic activation and toxicity for neurons. Further, they demostrated CD14 in Alzheimer's brains but not in control subjects by immunohistochemistry (Liu et al. 2005). Letiembre et al. showed an altered regulation of innate immune receptors in older nondemented people. Given that TLR4 is necessary to engage the innate immune responses in the brain (Fassbender et al. 2004; Letiembre et al. 2007; Liu et al. 2005), we had hypothesized that TLR4-mutant subjects will have fewer brain inflammatory responses. However, that was not the case; trafficking of inflammatory cells and accumulation of Aβ42 were also observed in the 3 TLR4-mutant subjects, thus suggesting that factors other than TLR4 are also playing a crucial role in cell trafficking and amyloid accumulation observed in these megacity pollution-exposed subjects.

We would like to propose that sustained exposures to significant levels of air pollutants including UFPM, $PM_{2.5}$, and PM-LPS produce brain neuroinflammation and neurode-generation through at least four pathways.

1. Induction of upper respiratory, lung epithelial, and endothelial injury leading to persistant chronic inflammation in the respiratory tract and systemic inflammation. The systemic imflammation is accompanied by the production of pro-inflammatory cytokines such as TNFα, IL-6 and IL-1β (all of which are upregulated in MC children), for which brain blood vessels exhibit constitutive and induced expression of receptors. These cytokines can activate endothelial cells in the BBB, disrupt the BBB (early findings in highly exposed subjects and dogs), upregulate COX2 (target brain regions in MC subjects), and trigger cascades leading to activation of MAP kinases/NFκB (nuclear transduction of NFκB in endothelial brain cells in exposed subjects). A high level of activation of NFκB in astrocytes results in increased expression of nitric oxide synthase (seen in three-month-old MC dogs), and nitric oxide production that opens the BBB (seen in dogs, children, and teens). The early disruption of the BBB is followed by leaking of RBC and proteins such as prothrombin (neurotoxic protease, increases APP) (Grammas et al. 2006; Mhatre et al. 2006; Zipser et al. 2007) and trafficking of inflammatory cells expressing CD163, CD68, and HLA-DR, as well as mast cells in keeping with the inflammatory response. A dysregulated inflammatory response involves neural-immune interactions including the upregulation of CD14 that further activate immune cells, glial cells, and neurons (Fassbender et al. 2004; Letiembre et al. 2007; Liu et al. 2005; Minghetti 2005). Chronic oxidative stress is an early component of the brain responses, as evidenced by DNA oxidative damage present in different target brain areas as well as outside the CNS (Calderón-Garcidueñas, Maronpot et al. 2003).

2. We strongly support the importance of the olfactory pathway, especially in children, since olfactory neurons are loaded with PM and a strong early upregulation of COX2, IL-1β, and CD14 is present. Early damage to the OB and its connections and the accumulation of Aβ42 and α-synuclein will potentially translate into an abnormality in the limbic system, including the hippocampus and the parahippocampal gyri, as well as a decrease in the number of stem cells existing in the OB (Bédard et al. 2004).

3. The vagus/trigeminal (Lewis et al. 2005) pathways are also crucial, given that PM enters the respiratory and digestive systems (i.e., the liver). PM-LPS is likely to play an important role in these pathways, as shown by the vagal upregulation of CD14.

4. Direct access of UFPM to the brain, further accentuating an inflammatory response in the brain parenchyma (ROS production in activated microglia and perivascular

macrophages), damaging components of the BBB, and potentially enhancing the rate of protein fibrillation affecting Aβ42 and α-synuclein (Linse et al. 2007).

All four pathways are clearly demonstrated in MC children, teens, and young adults, and based on the long-standing view that chronic inflammation, altered innate immune responses, and oxidative stress are detrimental, we propose that inflammatory interactions that take place at the blood-endothelium interface along with early oxidative stress are the bases for the early Alzheimer's and Parkinson's-like changes we observed in these populations. Oxidative stress in AD and PD is involved at the earlier stages of the pathological cascades with aggregation of the target proteins: amyloid β, tau and α-synuclein as an initial compensatory response (Eriksen et al. 2003; Fink 2006; Forero et al. 2006; Minghetti 2005; Nunomura et al. 2006; Quilty et al. 2006; Sidhu et al. 2004; Zhu et al. 2006). Persistance of the initial damaging factors translates into a neurodegenerative response.

In summary, exposure to significant concentrations of air pollutants including UFPM and $PM_{2.5}$ produces neuroinflammation and altered innate immune responses in crucial brain target anatomical areas in children and young adults. Ultrafine PM could play a role in the enhancement rate of protein fibrillation affecting Aβ42 and α-synuclein (Linse et al. 2007). We strongly propose that neuroinflammation as a result of exposure to air pollution could have a causative role in both Alzheimer's and Parkinson's diseases and that sustained brain inflammation confers a higher risk for the development of these two frequent neurodegenerative disorders. In the United States, 158 million people live in areas where $O_3$ exceeds the eight-hour standard, 29 million are exposed to $PM_{10}$, and 88 million are exposed to $PM_{2.5}$ (http://www.epa.gov/oar/oaqps/greenbk/03co.html). Neuroinflammation provides a mechanistic link between inhalation/ingestion of air pollutants and neurodegeneration as seen in AD and PD. Neuroinflammation and accumulation of Aβ42 and α-synuclein in key target brain areas start in healthy children with no known risk factors for neurodegenerative diseases. Long-term exposure to air pollution should be considered a risk factor for both Alzheimer's and Parkinson's diseases, and APOE ε 4 allele carriers could have a higher risk of developing AD if they reside in a polluted environment.

## Abbreviations

| | |
|---|---|
| **Aβ42** | beta amyloid |
| **AD** | Alzheimer's disease |
| **APO** | E apolipoprotein E |

| | |
|---|---|
| **APP** | amyloid precursor protein |
| **BBB** | blood-brain barrier |
| **COX2** | cyclooxygenase 2 |
| **GFAP** | glial fibrillary acidic protein |
| **HLA-DR** | human leukocyte antigen-DR |
| **IL-1β** | interleukin-1β |
| **ICAM-1** | intercellular adhesion molecule-1 |
| **IHC** | immunohistochemistry |
| **LPS** | lipopolysaccharide |
| **MC** | Mexico City |
| **MTBE** | methyl-ter-butyl ether |
| **NFκB** | transcription factor nuclear factor kappa-B |
| **NSE** | neuron specific enolase |
| **$O_3$** | ozone |
| **OB** | olfactory bulb |
| **PD** | Parkinson's disease |
| **PM** | particulate matter |
| **PNS** | peripheral nervous system |
| **PT** | prothrombin |
| **RBC** | red blood cells |
| **SNC** | substantia nigrae pars compacta |
| **TLR** | toll-like receptor |
| **UFPM** | ultrafine PM |
| **VCAM-1** | vascular adhesion molecule-1 |
| **ZO-1** | zonula occludens-1 |

## Footnotes

Author to whom requests for reprints should be addressed: William Reed, PhD, Center for Environmental Medicine, Asthma & Lung Biology CB#7310, University of North Carolina at Chapel Hill, 104 Mason Farm Road, Chapel Hill, NC 27599; e-mail: william_reed@med.unc.edu

---

This work was supported in part by the National Science Foundation 0346458, the Montana Board of Research and Commercialization Technology 04-06, 1KO1 NS046410-01A1, 1R21-ES013293-01, and 5 P20 RR015583 from the National Center for Research Resources (NCRR). Advice and support from Jerrold Abraham, MD, SUNY Upstate Medical University, a 

appreciated. We appreciate the technical assistance of Sarah Ulatowski and Rodolfo Villarreal-Calderón. Lilian Calderón-Garcidueñas and William Reed contributed equally to this work.

## References

1. Abbott NJ. 2005 Dynamics of CNS barriers: evolution, differentiation and modulation. *Cell Mol Neurobiol* 25:5-23

Crossref

PubMed

Google Scholar

---

2. Akiyama H, Barger S, Barnum S, Bradt B, Bauer J, Cole GM, et al. 2000 Inflammation and Alzheimer's disease. *Neurobiol Aging* 21:383-421

Crossref

PubMed

Web of Science

Google Scholar

---

3. Allan SM, Tyrrell PJ, and Rothwell NJ. 2005 Interleukin-1 and neuronal injury. *Nat Rev Immunol* 5:629-40

Crossref

PubMed

Web of Science

Google Scholar

---

4. Banauch GI, Hall C, Weiden M, Cohen HW, Aldrich TK, Christodoulou V, et al. 2006 Pulmonary function after exposure to the World Trade Center collapse in the New

department. *Am Respir Crit Care Med* 174:312-19

Crossref

PubMed

Google Scholar

---

5. Bédard A and Parent A. 2004 Evidence of newly generated neurons in the human olfactory bulb. *Dev Brain Res* 151:159-168

Crossref

PubMed

Google Scholar

---

6. Bennett WD and Zeman KL. 2005 Effect of race on fine particle deposition for oral and nasal breathing. *Inhal Toxicol* 17:641-48

Crossref

PubMed

Google Scholar

---

7. Benveniste EN. 1998 Cytokine actions in the central nervous system. *Cytokine Growth Factor Rev* 9:259-75

Crossref

PubMed

Web of Science

Google Scholar

---

8. Blamire AM, Anthony DC, Rajagopalan B, Sibson NR, Perry VH, and Styles P. 2000 Interleukin-1β-induced changes in blood-brain barrier permeability, apparent diffusion

coefficient, and cerebral blood volume in the rat brain: a magnetic resonance study. *J Neurosci* 20:8153-59

Crossref

PubMed

Google Scholar

---

9. Block ML, Wu X, Pei Z, Wang T, Qin L, Wilson B, et al. 2004 Nanometer size diesel exhaust particles are selectively toxic to dopaminergic neurons: the role of microglia, phagocytosis, and NADPH oxidase. *FASEB J* 18:1618-20

Crossref

PubMed

Web of Science

Google Scholar

---

10. Bonner JC, Rice AB, Lindroos PM, O'Brien PO, Dreher KL, Rosas I, et al. 1998 Induction of the lung myofibroblast PDGF receptor system by urban ambient particles from Mexico City. *Am J Respir Cell Mol Biol* 19:672-80

Crossref

PubMed

Web of Science

Google Scholar

---

11. Braak H, de Vos RAI, Bohl J, and Del Tredeci K. 2006 Gastric α synuclein immunoreactive inclusions in Meissner's and Auerbach's plexuses in cases staged for Parkinson's disease-related brain pathology. *Neurosci Lett* 396:67-76

Crossref

PubMed

Google Scholar

12. Braak H, Rub U, Gai WP, and Del Tredeci K. 2003 Idiopathic Parkinson's disease: possible routes by which vulnerable neuronal types may be subject to neuroinvasion by an unknown pathogen. *J Neural Transm* 110:517-36

Crossref

PubMed

Web of Science

Google Scholar

13. Bravo-Alvarez HR and Torres-Jardón R. Fenn M, de Bauer L, and Hernández T. 2002 Air pollution levels and trends in the México City metropolitan area. *Urban Air Pollution and Forest: Resources at Risk in the Mexico City Air Basin* Ecological Studies. 156:121-59 Springer-Verlag New York, USA

Crossref

Google Scholar

14. Brett FM, Mizisin AP, Powell HC, and Campbell IL. 1995 Evolution of neuropathologic abnormalities associated with blood-brain-barrier breakdown in transgenic mice expressing interleukin-6 in astrocytes. *J Neuropath Exp Neurol* 54:766-75

Crossref

PubMed

Google Scholar

15. Brunekreef B and Holgate ST. 2002 Air pollution and health. *Lancet* 360:1233-42

Crossref

PubMed

Web of Science

Google Scholar

16. Calderón-Garcidueñas L, Valencia-Salazar G, Rodríguez-Alcaraz A, Gambling T, Garcia R, Osnaya N, et al. 2001 Ultrastructural nasal pathology in children chronically and sequentially exposed to air pollutants. *Am J Respir Crit Care Med* 24:132-38

Google Scholar

17. Calderón-Garcidueñas L, Mora-Tiscareño A, Fordham LA, Chung CJ, Garcia R, Osnaya N, et al. 2001 Canines as sentinel species for assessing chronic exposures to air pollutants. *Toxicol Sci* 61:342-67

Crossref

PubMed

Google Scholar

18. Calderón-Garcidueñas L, Azzarelli B, Acuña H, García R, Gambling TM, Osnaya N, et al. 2002 Air Pollution and Brain Damage. *Toxicol Pathol* 30:373-89

Crossref

PubMed

Web of Science

Google Scholar

19. Calderón-Garcidueñas L, Maronpot RR, Torres-Jardon R, Henríquez-Roldán C, Schoonhoven R, Acuña–Ayala H, et al. 2003 DNA damage in nasal and brain tissues of canines exposed to air pollutants is associated with evidence of chronic brain inflammation and neurodegeneration. *Toxicol Pathol* 31:524-38

Crossref

PubMed

Web of Science

Google Scholar

20. Calderón-Garcidueñas L, Mora-Tiscareño A, Fordham LA, Valencia-Salazar G, Chung CJ, Rodríguez-Alcaraz A, et al. 2003 Respiratory damage in children exposed to urban pollution. *Pediatr Pulmonol* 36:148-61

Crossref

PubMed

Web of Science

Google Scholar

21. Calderón-Garcidueñas L, Reed W, Maronpot RR, Henriquez-Roldan C, Delgado-Chavez R, Calderón-Garcidueñas A, et al. 2004 Brain inflammation and Alzheimer's-like pathology in individuals exposed to severe air pollution. *Toxicol Pathol* 32:650-58

Crossref

PubMed

Web of Science

Google Scholar

22. Calderón-Garcidueñas L, Hazucha MJ, Herbst MC, Cascio WE, and Reed W. 2006 Supraventricular arrhythmias, cardiac vagal tone, and endothelin-1 (ET-1) in children exposed to severe urban air pollution. *Proc Am Thorac Soc* 3 abstracts issue A46, April 2006.

Google Scholar

23. Calderón-Garcidueñas L, Franco-Lira M, Torres-Jardon R, Henríquez-Roldán C, Barragan-Mejía G, Valencia-Salazar G, et al. 2007 Pediatric respiratory and systemic effects of chronic air pollution exposure: nose, lung, heart, and brain pathology. *Toxicol Pathol* 35:1-9

Crossref

Google Scholar

24. Calderón-Garcidueñas L, Vincent R, Mora-Tiscareño A, Franco-Lira M, Henríquez-Roldán C, Barragan-Mejía G, et al. 2007 Elevated plasma Endothelin-1 and Pulmonary arterial pressure in children exposed to air pollution. *Environ Health Perspect* 115:1248-53

Crossref

PubMed

Web of Science

Google Scholar

25. Choi SH, Langenbach R, and Bosetti F. 2006 Cyclooxygenase-1 and 2 enzymes differentially regulate the brain upstream NF-κB pathway and downstream enzymes involved in prostaglandin biosynthesis. *J Neurochem* 98:801-11

Crossref

PubMed

Google Scholar

26. Cunningham C, Wilcockson DC, Campion S, Lunnon K, and Perry VH. 2005 Central and systemic endotoxin challenges exacerbate the local inflammatory response and increase neuronal death during chronic neurodegeneration. *J Neurosci* 25:9275-84

Crossref

PubMed

Web of Science

Google Scholar

27. Daigle CC, Chalupa DC, Gibb FR, Morrow PE, Oberdorster G, Utell MJ, et al. 2003 Ultrafine particle deposition during rest and exercise. *Inhal Toxicol* 15:539-52

Crossref

PubMed

Google Scholar

28. Del Tredeci K, Rub U, de Vos RAI, Bohl JRE, and Braak H. 2002 Where does Parkinson's disease pathology begin in the brain?. *J Neuropath Exp Neurol* 61:413-26

Crossref

PubMed

Google Scholar

29. Djaldetti R, Ziv I, and Melamed E. 2006 The mystery of motor asymmetry in Parkinson's disease. *Lancet Neurol* 5:796-802

Crossref

PubMed

Web of Science

Google Scholar

30. Donaldson K. 2003 The biological effects of coarse and fine particulate matter. *Occup Environ Med* 60:313-14

Crossref

PubMed

Google Scholar

31. Dorman DC, Brenneman KA, McElveen AM, Lynch SE, Roberts KC, and Wong BA. 2002 Olfactory transport: a direct route of delivery of inhaled manganese phosphate to the rat brain. *J Toxicol Environ Health* 65:1493-1511

Crossref

Google Scholar

32. Dropp JJ. 1979 Mast cells in the human brain. *Acta Anat* 105:505-13

Crossref

PubMed

Google Scholar

33. Elmquist JK, Scammell TE, and Saper CB. 1997 Mechanisms of CNS response to systemic immune challenge: the febrile response. *Trends Neurosci* 20:565-70

Crossref

PubMed

Web of Science

Google Scholar

34. Eriksen JL, Dawson TM, Dickson DW, and Petrucelli L. 2003 Caught in the act: α synuclein is the culprit in Parkinson's disease. *Neuron* 40:453-56

Crossref

PubMed

Google Scholar

35. Farkas E, Süle Z, Tóth-Szu ''ki V, Mátyás A, Antal P, Farkas IG, et al. 2006 Tumor necrosis factor-alpha increases cerebral blood flow and ultrastructural capillary damage through the release of nitric oxide in the rat brain. *Microvasc Res* 72:113-19

Crossref

PubMed

Web of Science

Google Scholar

36. Fassbender K, Walter S, Kuhl S, Landmann R, Ishii K, Bertsch T, et al. 2004 The LPS receptor (CD14) links innate immunity with Alzheimer's disease. *FASEB J* 18:203-5

Crossref

PubMed

Google Scholar

37. Ferrari CC, Pott-Godoy MC, Tarelli R, Chertoff M, Depino AM, and Pitossi FJ. 2006 Progressive neurodegeneration and motor disabilities induced by chronic expression of IL-1 beta in the substantia nigrae. *Neurobiol Dis* 24:183-93

Crossref

PubMed

Google Scholar

38. Fink AL. 2006 The aggregation and fibrillation of alpha-synuclein. *Acc Chem Res* 39:628-34

Crossref

PubMed

Google Scholar

39. Forero DA, Casadesus G, Perry G, and Arboleda H. 2006 Synaptic dysfunction and oxidative stress in Alzheimer's disease: emerging mechanisms. *J Cell Mol Med* 10:796-805

Crossref

PubMed

Web of Science

Google Scholar

40. Geiser M, Rothen-Rutishauser B, Kapp N, Schurch S, Kreyling W, Schulz H, et al. 2005 Ultrafine particles cross cellular membranes by nonphagocytic mechanisms in lungs and in cultured cells. *Environ Health Perspect* 113:1555-60

Crossref

PubMed

Web of Science

Google Scholar

41. Goehler LE, Gaykema R, Nguyen K, Hansen M, Maier SF, and Watkins LR. 1999 Interleukin-1 beta in immune cells of the abdominal vagus nerve: a link between the immune and nervous systems?. *J Neurosci* 19:2799-806

Crossref

PubMed

Google Scholar

42. Grammas P, Samany PG, and Thirumangalakudi L. 2006 Thrombin and inflammatory are elevated in Alzheimer's disease microvessels: implications for disease pathogenesis. *J Alzheimers Dis* 9:51-58

Crossref

PubMed

Google Scholar

43. Griffin WS and Mrak RE. 2002 Interleukin-1 in the genesis and progression of and risk for development of neuronal degeneration in Alzheimer's disease. *J Leukoc Biol* 72:233-38

Crossref

PubMed

Web of Science

Google Scholar

44. Hawkes C. 2003 Olfaction in neurodegenerative disorders. *Mov Disord* 18:364-72

Crossref

PubMed

Google Scholar

45. Henriksson J, Tallkvist J, and Tjalve H. 1997 Uptake of nickel into the brain via olfactory neurons in rats. *Toxicol Lett* 91:153-62

Crossref

PubMed

Web of Science

Google Scholar

46. Hickey WF. 2001 Basic principles of immunological surveillance of the normal central nervous system. *Glia* 36:118-24

Crossref

PubMed

Web of Science

Google Scholar

47. Ibrahim MZM, Reder AT, Lawand R, Takash W, and Sallouh-Khatib S. 1996 The mast cells of the multiple sclerosis brain. *J Neuroimmunol* 70:131-38

Crossref

PubMed

Web of Science

Google Scholar

48. Jellinger KA. 2003 Neuropathological spectrum of Synucleopathies. *Mov Disord* 18:S2-S12

Crossref

PubMed

Google Scholar

49. Kim WK, Alvarez X, Fisher J, Bronfin B, Westmoreland S, McLaurin J, et al. 2006 CD163 identifies perivascular macrophages in normal and viral encephalitic brains and potential precursors to perivascular macrophages in blood. *Am J Pathol* 168:822-34

Crossref

PubMed

Web of Science

Google Scholar

50. Kukanova B and Mravec B. 2006 Complex intracardiac nervous system. *Bratisl Lek Listy* 107:45-51

PubMed

Google Scholar

51. Kurosinski P, Guggisberg M, and Gotz J. 2002 Alzheimer's and Parkinson's disease-overlapping or synergistic pathologies?. *Trends Mol Med* 8:3-5

Crossref

PubMed

Google Scholar

52. Letiembre M, Hao W, Liu Y, Walter S, Mihaljevic I, Rivest S, et al. 2007 Innate immune receptor in normal brain aging. *Neuroscience* 146:248-54

Crossref

PubMed

Google Scholar

53. Lewis J, Bench G, Myers O, Tinner B, Staines W, Barr E, et al. 2005 Trigeminal uptake and clearance of inhaled manganese chloride in rats and mice. *Neurotox* 26:113-23

Crossref

Google Scholar

54. Linse S, Cabaleiro-Lago C, Xue WF, Lynch I, Lindman S, Thulin E, et al. 2007 Nucleation of protein fibrillation by nanoparticles. *Proc Natl Acad Sci USA* 104:8691-96

Crossref

PubMed

Web of Science

Google Scholar

55. Liu Y, Walter S, Stagi M, Cherny D, Letiembre M, Schuz-Schaeffer W, et al. 2005 LPS receptor (CD14): a receptor for phagocytosis of Alzheimer's amyloid peptide. *Brain* 128:1778-89

Crossref

PubMed

Web of Science

Google Scholar

56. Lossinsky AS and Shivers RR. 2004 Structural pathways for macromolecular and cellular transport across the blood brain barrier during inflammatory conditions. Review. *Histol Histopath* 19:535-64

PubMed

Google Scholar

57. McGeer PL, Rogers J, and McGeer EG. 2006 Inflammation, anti-inflammatory agents and Alzheimer's disease: the last 12 years. *J Alzheimers Dis* 9:271-76

Crossref

PubMed

Google Scholar

58. McQueen DS, Donaldson K, Bond SM, McNeilly JD, Newman S, Barton NJ, et al. 2007 Bilateral vagotomy or atropine pre-treatment reduces experimental diesel-soot induced lung inflammation. *Toxicol Appl Pharmacol* 219:62-71

Crossref

PubMed

Google Scholar

59. Mexico City Ambient Air Monitoring Network. http://www.sma.df.gob.mx/simat.

Google Scholar

60. Mhatre M, Hensley K, Nguyen A, and Grammas P. 2006 Chronic thrombin exposure results in an increase in apolipoprotein-E levels. *J Neurosci Res* 84:444-49

Crossref

PubMed

Google Scholar

61. Minghetti L. 2005 Role of inflammation in neurodegenerative diseases. *Curr Opinion Neu* 18:315-21

Crossref

PubMed

Google Scholar

62. Moynagh PN. 2005 The interleukin-1 signalling pathway in astrocytes: a key contributor to inflammation in the brain. *J Anat* 207:265-69

Crossref

PubMed

Google Scholar

63. Nadeau S and Rivest S. 1999 Effects of circulating tumor necrosis factor on the neuronal activity and expression of the genes encoding the tumor necrosis factor receptors (p55 and p75) in the rat brain: a view from the blood-brain barrier. *Neuroscience* 93:1449-64

Crossref

PubMed

Web of Science

Google Scholar

64. Nguyen MD, Julien JP, and Rivest S. 2002 Innate immunity: the missing link in neuroprotection and neurodegeneration?. *Nat Rev Neurosci* 3:216-27

Crossref

PubMed

Web of Science

Google Scholar

65. Nolan JP. 1975 The role of endotoxin in liver injury. *Gastroenterology* 69:1346-56

Crossref

PubMed

Web of Science

Google Scholar

66. Nunomura A, Castellani RJ, Zhu X, Moreira PI, Perry G, and Smith MA. 2006 Involvement of oxidative stress in Alzheimer's disease. *J Neuropath Exp Neurol* 65:631-41

Crossref

PubMed

Google Scholar

67. Oberdorster G, Sharp Z, Atudorel V, Elder A, Gelein R, Lunts A, et al. 2002 Extrapulmonary translocation of ultrafine carbon particles following whole-body inhalation exposure of rats. *J Toxicol Environ Health* 65:1531-43

Crossref

Google Scholar

68. Pahl HL. 1999 Activators and target genes of Rel/NF-kappa B transcription factors. *Oncogene* 18:6853-66

Crossref

PubMed

Google Scholar

69. Pan W and Kastin AJ. 2001 Upregulation of the transport system for TNF-α at the blood-brain barrier. *Arch Physiol Biochem* 109:350-53

PubMed

Google Scholar

70. Persson J, Lind J, Larsson A, Ingvar M, Cruts M, Van Broeckhoven C, et al. 2006 Altered brain white matter integrity in healthy carriers of the APOE ε4 allele. A risk for AD?. *Neurology* 66:1029-33

Crossref

PubMed

Google Scholar

71. Peters A, Veronesi B, Calderón-Garcidueñas L, Gehr P, Chi Chen L, Geiser M, et al. 2006 Translocation and potential neurological effects of fine and ultrafine particles: a critical update. *Part Fiber Tox* 3:1-13

Crossref

PubMed

Google Scholar

72. Qin W, Ho L, Pompl PN, Peng Y, Zhao Z, Xiang Z, et al. 2003 Cyclooxygenase (COX)-2 and COX1 potentiate β-amyloid peptide generation through mechanisms that involve γ-secretase activity. *J Biol Chemistry* 51:50970-77

Crossref

Google Scholar

73. Quilty MC, King AE, Gai WP, Pountney DL, West AK, Vickers JC, et al. 2006 Alpha-synuclein is upregulated in neurons in response to chronic oxidative stress and is associated

neuroprotection. *Exp Neurol* 199:249-56

Crossref

PubMed

Google Scholar

74. Rivest S. 2001 How circulating cytokines trigger the neural circuits that control the hypothalamic-pituitary-adrenal axis. *Psychoneuroendocrinology* 26:761-88

Crossref

PubMed

Web of Science

Google Scholar

75. Rothen-Rutishauser BM, Schurch S, Haenni B, Kapp N, and Gehr P. 2006 Interaction of fine particles and nanoparticles with red blood cells visualized with advanced microscopic techniques. *Environ Sci Technol* 40:4353-59

Crossref

PubMed

Google Scholar

76. Rothwell NJ and Luheshi GN. 2000 Interleukin-1 in the brain: biology, pathology and therapeutic target. *Trends Neurosci* 23:618-25

Crossref

PubMed

Google Scholar

77. Selkoe DJ. 2002 Alzheimer's disease is a synaptic failure. *Science* 298:789-91

Crossref

PubMed

Web of Science

Google Scholar

78. Selkoe DJ. 2001 Alzheimer's disease: genes, proteins, and therapy. *Physiol Rev* 81:741-66

Crossref

PubMed

Web of Science

Google Scholar

79. Sidhu A, Wersinger C, Moussa CE, and Vernier P. 2004 The role of alpha synuclein in both neuroprotection and neurodegeneration. *Ann NY Acad Sci* 1035:250-70

Crossref

PubMed

Google Scholar

80. Simard AR and Rivest S. 2006 Neuroprotective properties of the innate immune system and bone marrow stem cells in Alzheimer's disease. *Mol Psychiatry* 11:327-35

Crossref

PubMed

Google Scholar

81. Theoharides TC. 1990 Mast cells: the immune gate to the brain. *Life Scien* 46:607-17

Crossref

PubMed

Google Scholar

82. Thiel VE and Audus KL. 2001 Nitric oxide and blood brain barrier integrity. *Antioxid Redox Signal* 3:273-78

Crossref

PubMed

Google Scholar

83. Thomson E, Goegan P, Kumarathasan P, and Vincent R. 2004 Air pollutants increase gene expression of the vasoconstrictor endothelin-1 in the lungs. *Biochem Biophys Acta* 1689:75-82

PubMed

Google Scholar

84. Thomson E, Kumarathasan P, Goegan P, Aubin RA, and Vincent R. 2005 Differential regulation of the lung endothelin system by urban particulate matter and ozone. *Toxicol Sci* 88:103-13

Crossref

PubMed

Google Scholar

85. Tripathi AK, Sullivan DJ, and Stins MF. 2006 Plasmodium falciparum-infected erythrocytes increase intercellular adhesion molecule 1 expression on brain endothelium through NF-κB. *Infect Immun* 74:3262-70

Crossref

PubMed

Google Scholar

86. Uyama N, Geerts A, and Reynaert H. 2004 Neural connections between the hypothalamus and the liver. *Anat Rec A Discover Mol Cell Evol Biol* 280:808-20

Crossref

PubMed

Google Scholar

87. Villarreal-Calderón A, Acuña H, Villarreal-Calderón J, Garduño M, Henríquez-Roldán CF, Calderón-Garcidueñas L, et al. 2002 Assessment of physical education time and after-school outdoor time in elementary and middle school students in south Mexico City: the dilemma between physical fitness and the adverse health effects of outdoor pollutant exposure. *Arch Environ Health* 57:450-60

Crossref

PubMed

Google Scholar

88. Wake K, Decker K, Kim A, Knook DL, McCuskey RS, Bouwens L, et al. 1989 Cell biology and kinetics of Kupffer cells in the liver. *Int Rev Cytol* 118:173-229

Crossref

PubMed

Google Scholar

89. Wishart HA, Saykin AJ, McAllister TW, Rabin LA, McDonald BC, Flashman LA, et al. 2006 Regional brain atrophy in cognitively intact adults with a single APOE ε4 allele. *Neurol* 67:1221-24

Crossref

PubMed

Google Scholar

90. Xiang Z, Ho L, Yemul S, Zhao Z, Qing W, Pompl P, et al. 2002 Cyclooxygenase 2 promotes amyloid plaque deposition in a mouse model of Alzheimer's disease neuropathology. *Gene Exp* 10:271-78

Crossref

PubMed

Google Scholar

91. Xiao G, Rabson AB, Young W, Qing G, and Qu Z. 2006 Alternative pathways of NF-κB activation: A double-edged sword in health and disease. *Cytokine Growth Factor Rev* 17:281-93

Crossref

PubMed

Google Scholar

92. Zhang J and Rivest S. 2003 Is survival possible without arachidonate metabolites in the brain during systemic infection?. *News Physiol Sci* 18:137-42

Crossref

PubMed

Google Scholar

93. Zhu X, Perry G, Moreira PI, Aliev AD, Hirai K, and Smith VA. 2006 Mitochondrial abnormalities and oxidative imbalance in Alzheimer's disease. *J Alzheimers Dis* 9:147-53

Crossref

PubMed

Google Scholar

94. Zipser BD, Johanson CE, Gonzalez L, Berzin TM, Tavares R, Hulette CM, et al. 2007 Microvascular injury and blood-brain-barrier leakage in Alzheimer's disease. *Neurobiol Aging* 28:977-86

Crossref

PubMed

Google Scholar

## Figures and Tables

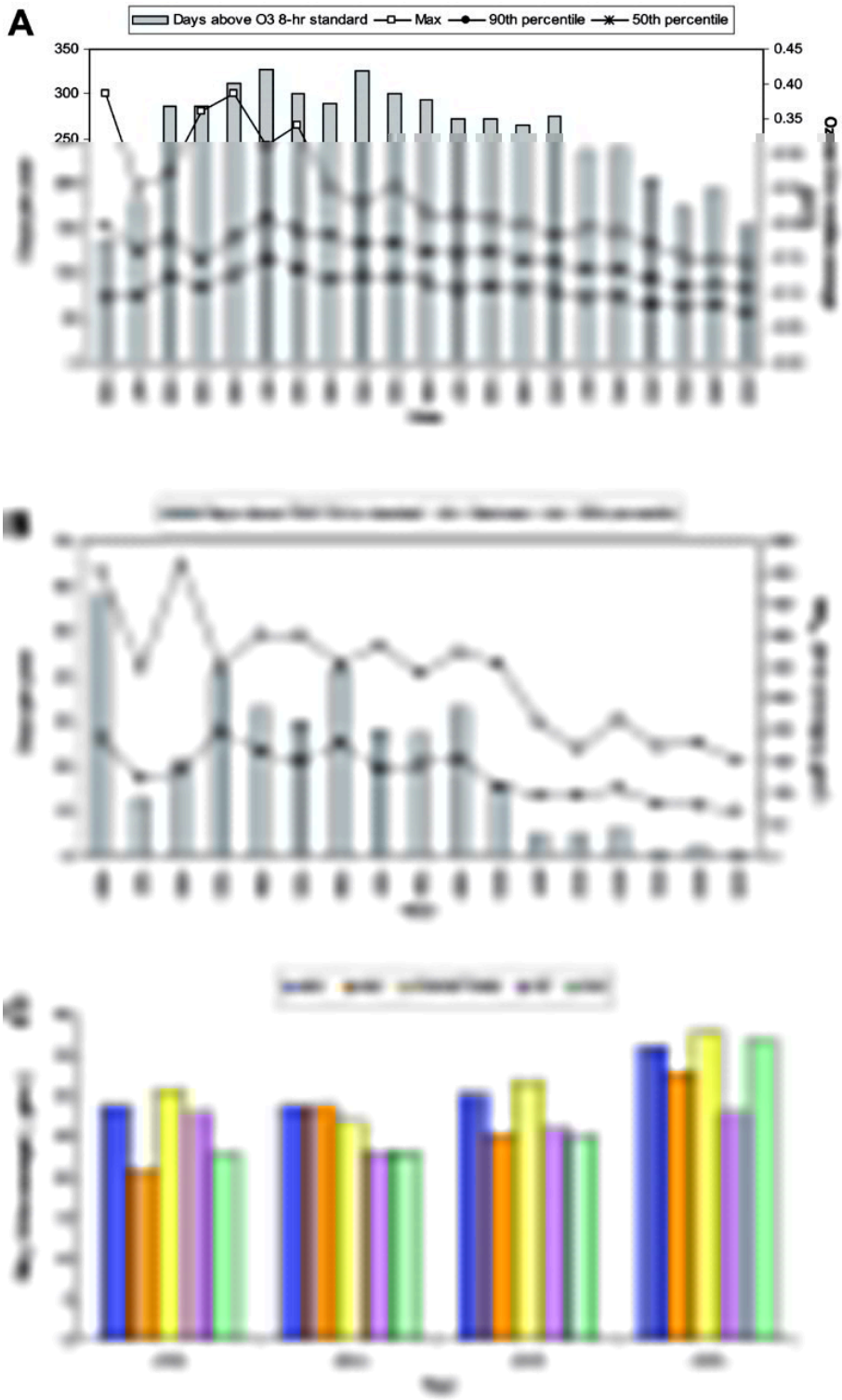


**Figure 1** A. Ozone eight-hour mobile average concentrations for Mexico City (MC) for the years 1986–2006. We illustrate the variations in the yearly number of days above the $O_3$ eight-hour mobile average air quality standard (0.08 ppm), the maximum, and the 90th and the 50th percentiles registered in all the $O_3$ monitoring sites in MC.

B. $PM_{10}$ exceedences above the twenty-four-hour air quality standard (150 $\mu g/m^3$) for MC for the years 1990–2006 and the variations in maximum and 50th percentiles of the whole $PM_{10}$ da

average levels registered in all the MC $PM_{10}$ monitoring sites during the same period.

---

C. $PM_{2.5}$ twenty-four-hour and annual average concentrations for five different regions in MC for the years 2003–2006. All five regions including downtown, NW, NE, SW, and SE have annual average concentrations of $PM_{2.5}$ above the respective annual standard (15 $\mu g/m^3$). (All graphs constructed with data available from the Mexico City Ambient Air Monitoring Network, http://www.sma.df.gob.mx/simat)

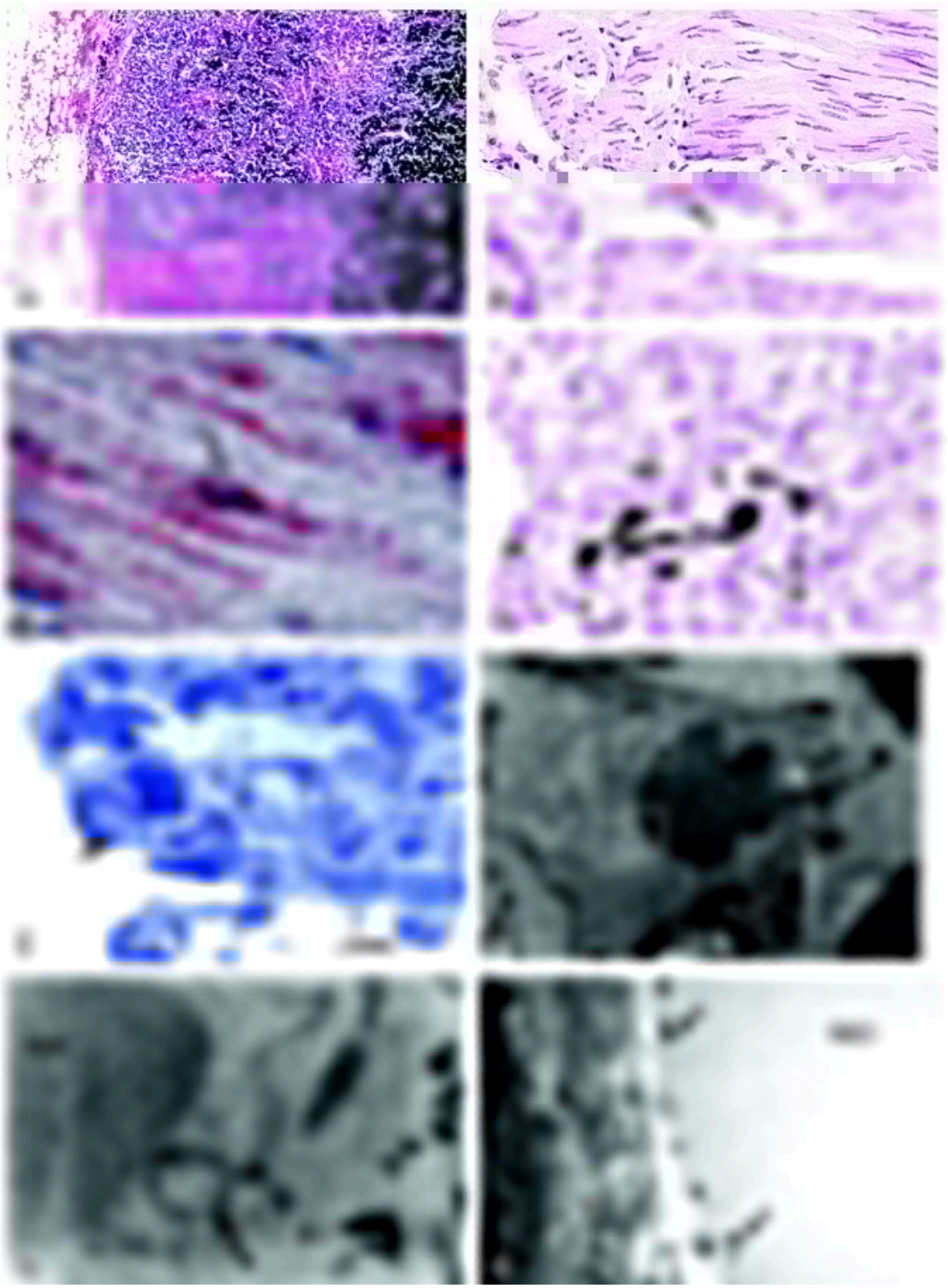

**Figure 2** A. Peribronchial lymph node in a seventeen-year-old male MC nonsmoker. There are numerous macrophages in the cortical zone loaded with black particulate matter. The afferent lymphatics also exhibit abundant PM-loaded macrophages.

B. Bronchial ganglion cells with positive α-synuclein granular punctuate cytoplasmic deposits (arrow) (brown product). (α-synuclein IHC)

C. Mexico City eleven-year-old boy APOE ε 3/3 exhibits granular punctuate deposits in the cytoplasm of Schwann cells in parenchymal lung nerves (arrow) (red product). (α-synuclein IHC)

D. Kupffer cells loaded with PM in the liver of a thirty-two-year-old MC resident. (Hematoxylin stain)

E. One-micron toluidine blue section of lung in a thirty-three-year-old male MC resident. PMNs are seen attached to endothelial cells (arrow) in lung capillaries, in keeping with endothelial activation and the significant decrease of circulating PMNs observed in young MC residents. (Toluidine blue 1-µm section)

F. Electron micrographs of lung capillaries in a twenty-four-year-old female MC resident. The endothelial cell lining of the lung capillary exhibits elongated fronds that surround a luminal erythrocyte. The endothelial fronds completely embrace the erythrocyte on the plane of the picture. The inserts display the close association between the cytoplasm of the endothelial cell and the erythrocyte, with aggregation of particulate material at the interphase. (EM x 12,000 inserts x 25,000)

G. Same lung capillary as Figure 2F, showing the relationship between the endothelial cell membrane-bound structure (arrow) with ultrafine PM and the erythrocyte (RBC) surface. (EM x 50,000)

H. An erythrocyte (RBC) in the lumen of a lung capillary exhibits numerous nanosized particulate material. EC is the endothelial cell. (EM x 50,000)

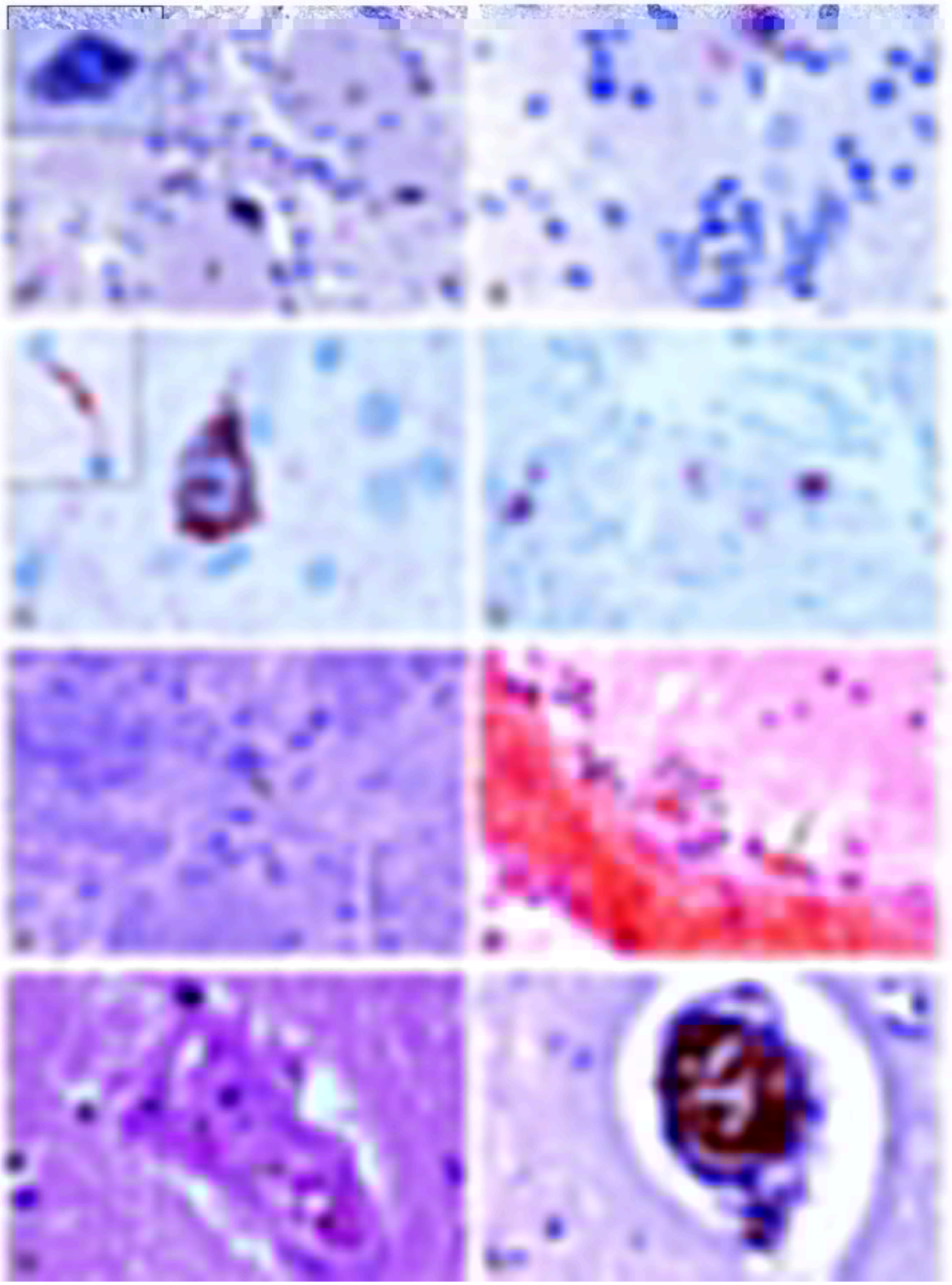

**Figure 3** A. Olfactory bulb (OB) neurons (enolase-positive) in the glomerular region (g) exhibit abundant particulate matter (PM) in their cytoplasm in a fourteen-year-old Mexico City (MC) boy. Upper-left insert: a close-up of one PM-loaded neuron with positive Aβ42 red product in its cytoplasm. (Aβ42 IHC counterstained with hematoxylin)

B. OB in an eleven-year-old MC boy APOE β 3/3 showing Aβ42 immunoreactivity in glial cells (arrow, red product). The blood vessel (bv) in the lower central area is free of amyloid. (Aβ42 IHC

counterstained with H)

C. Olfactory bulb in a forty-two-year-old MC male, α-synuclein granular positive neurons are seen along Lewy neurites (insert).

D. OB in the same eleven-year-old boy as Figure 3B showing granular positive staining for α-synuclein in olfactory neurons (enolase-positive, not shown). (α-synuclein IHC)

E. One-micron toluidine blue section from a trigeminal ganglia in a twenty-year-old MC male. A partially degranulated mast cell (arrow) is seen in the perineural space. (Toluidine blue 1μm section)

F. Frontal white matter blood vessel in a thirty-two-year-old MC female. The blood vessel shows numerous hemosiderin-laden perivascular macrophages (arrow) and mononuclear cells. (H & E stain)

G. Frontal cortex vessel from a seventeen-year-old MC boy with platelet thrombi (arrow) partially obstructing its lumen. (H & E stain)

H. A frontal blood vessel from an eleven-year-old MC boy exhibits positive prothrombin reaction within the vessel lumen (bv) and in extravascular location, including positive perivascular macrophages (arrow). (PT IHC counterstained with H)

**Figure 4** A. Entorhinal area (Broadman 28) blood vessel (bv) with significant number of perivascular mononuclear cells (arrow) in a twenty-two-year-old female from Mexico City (MC). (H & E stain)

B. Frontal white matter from a fourteen-year-old MC male stained with anti-CD163 antibody shows CD163 immunoreactivity in perivascular cells (long arrow) and microglia-like cells scattered in the neuropil (short arrows) (DAB, brown product). (CD163 IHC)

C. Frontal white matter in a twenty-four-year-old MC male. There are several strongly CD 68 positive perivascular cells (arrows), as well as scattered positive microglia-like cells (DAB, brown product). (CD68 IHC)

D. Midbrain bv showing strongly positive staining for HLA-DR in perivascular cells (arrow) in a thirty-four-year-old MC male. (HLA-DR IHC)

E. Frontal cortex in a twenty-four-year-old MC male showing perivascular bv tryptase + partially degranulated mast cells (arrow) (DAB, brown product). (Tryptase IHC)

F. Midbrain bv in a twenty-five-year-old MC male showing strong expression of VCAM-1 in endothelial cells (arrow) (DAB, brown product). (VCAM-1 IHC)

G. Frontal cortex in a twenty-four-year-old MC male stained with anti-3 nitrotyrosine (NT) antibody. Positive macrophage-like cells (arrow) are positive in the perivascular spaces (Fast Red, red product). (NT IHC)

H. Frontal white matter capillary in a fifteen-year-old MC boy showing strong nuclear endothelial expression (arrow) for NFκB. An adjacent glial cell exhibits weak staining in the cytoplasm (DAB, brown product). (NFκB Aminoterminal domain p65 IHC)

**Figure 5** A. Frontal cortex in an APOE β 3/3 seventeen-year-old Mexico City (MC) boy. A diffuse amyloid plaque is seen (arrow, red product). A stain for glial fibrillary acidic protein (GFAP) for reactive astrocytes is negative (brown product) (Fast Red, red product; and DAB, brown product). (Dual immunohistochemistry for Aβ42 and GFAP)

B. Frontal cortex in a thirty-six-year-old APOE 3/4 MC male with leaking blood vessels (short arrow) and mature Aβ42 plaques (long arrow, red product). Reactive astrocytes are numerous (cytoplasmic GFAP+) (brown product) (Fast Red, red product; and DAB, brown product). (Dual IHC for Aβ42 and GFAP)

C. Confocal micrograph of a frontal cortical blood vessel in an eleven-year-old stained with antibodies against Zonula occludens-1 (ZO-1). ZO-1 stains microvascular tight junctions (TJ). Vessels exhibit areas with discontinuous or punctate TJ staining (arrow).

D. Frontal white matter blood vessel in a twenty-year-old MC male, a dual staining for glucose transporter type 1 Glut1 (green product, endothelial cells), and CD163-positive perivascular macrophages (red product). (Dual staining for Glut 1 and CD163)

E. Seventeen-year-old MC boy midbrain section showing a gigantocellular reticular nucleus neuron (long arrow), strongly positive for 8-hydroxydeoxyguanosine adjacent to a leaky blood vessel with a weak positive endothelial cell (short arrow) (Fast Red, red product). (8-hydroxydeoxyguanosine IHC)

F. Substantia nigrae pars compacta pigmented neuron in an eleven-year-old MC boy showing a few neuromelanin granules (short arrow, black granules) and α-synuclein-positive granular stain (long arrow, red product) (Fast Red, red product). (α-synuclein IHC)

G. Frontal cortex capillary electron micrograph in a twenty-seven-year-old MC male. A RBC with ultrafine particles in its cytoplasm is seen forming discrete contact with the endothelial cell (EC) cytoplasm. Aggregation of intramembrane particles is seen at both the interphase between the RBC and the endothelial cell (arrow) and between the mononuclear cell (M) outside the blood-brain barrier (BBB) and the capillary. (EM X 12000)

H. Electron micrographs of a trigeminal ganglia capillary in a nineteen-year-old MC male shows the presence of discrete contact regions (arrow head) between the luminal RBC with ultrafine particles in its cytoplasm and the endothelial cell. The area of the contact region (arrow) between the RBC and the EC is shown on the right frame picture. (EM X 12000 and 30000)

**Table 1** Results of APOE and TLR4 genotyping, Aβ 42 and α-synuclein immunoreactivity by immunohistochemistry, disruption of the BBB as shown by abnormal ZO-1 tight junctions, and trafficking of inflammatory cells expressing CD163, CD68, and HLA-DR in Controls and Mexico City residents younger than 25 years.

| Genotype APOE TLR4 | Age/gender | Residency | Aβ42 immunoreactivity (OB, frontal, hippocampus) | α-synuclein immunoreactivity (OB, brain stem) | Disruption of the BBB (abnormal ZO-1) |
|---|---|---|---|---|---|
| APOE 3/3 TLR4 + | 2y M | MC | — | — | yes |
| APOE 3/3 TLR4 + | 2y F | Control | — | — | no |
| APOE 3/3 TLR4 + | 7y M | MC | — | — | no |
| APOE 3/3 TLR4 + | 11y M | MC | OB, frontal | OB | yes |

| Genotype APOE TLR4 | Age/gender | Residency | Aβ42 immunoreactivity (OB, frontal, hippocampus) | α-synuclein immunoreactivity (OB, brain stem) | Disruption of the BBB (abnormal ZO-1) |
|---|---|---|---|---|---|
| APOE 3/3 TLR4 + | 14y M | MC | OB, frontal | — | yes |
| APOE 3/3 TLR4 + | 15y M | MC | OB | — | yes |
| APOE 3/3 TLR4 + | 16y M | MC | frontal | — | yes |
| APOE 3/3 TLR4 + | 17y M | Control | — | — | no |
| APOE 3/3 TLR4 + | 17y M | Control | — | — | no |
| APOE 3/3 TLR4 + | 17y M | MC | frontal | OB spinal lemniscus | yes |
| APOE 3/3 TLR4 + | 17y M | MC | OB, frontal diffuse plaques | SNC | yes |
| APOE 3/3 TLR4 + | 17y M | Control | — | — | no |
| APOE 3/3 TLR4 + | 19y M | MC | — | — | yes |
| APOE 3/3 TLR4 + | 20y M | MC | — | OB | yes |
| APOE 3/3 TLR4 + | 20y M | MC | — | — | yes |
| APOE 3/3 TLR4 + | 21y F | Control | — | — | no |

| Genotype APOE TLR4 | Age/gender | Residency | Aβ42 immunoreactivity (OB, frontal, hippocampus) | α-synuclein immunoreactivity (OB, brain stem) | Disruption of the BBB (abnormal ZO-1) |
|---|---|---|---|---|---|
| APOE 3/3 TLR4 – | 22y F | MC | — | — | yes |
| APOE 3/3 TLR4 – | 22y F | MC | frontal | — | yes |
| APOE 3/3 TLR4 + | 22y F | MC | OB, frontal | — | yes |
| APOE 3/3 TLR4 + | 24y F | Control | — | — | no |
| APOE 3/3 TLR4 + | 24y M | MC | OB, frontal, hippocampus | — | yes |
| APOE 3/3 TLR4 + | 24y M | MC | frontal | — | yes |
| APOE 3/3 TLR4 + | 24y M | MC | — | — | yes |

Abbreviations: Aβ42, beta amyloid; APOE, apolipoprotein E; BBB, blood-brain barrier; HLA-DR, human leukocyte antigen-DR; MC, Mexico City; OB, olfactory bulb; SNC, substantia nigrae pars compacta; TLR, toll-like receptor; ZO-1, zonula occludens-1.

**Table 2** Results of APOE and TLR4 genotyping, Aβ42 and α-synuclein immunoreactivity by immunohistochemistry, disruption of the BBB as shown by abnormal ZO-1 tight junctions, and trafficking of inflammatory cells expressing CD163, CD68, and HLA-DR in Controls and Mexico City residents older than 25 years.

| Genotype (APOE TLR4) | Age/gender | Residency | Aβ42 immunoreactivity (OB, frontal, hippocampus) | α-synuclein immunoreactivity (OB, brain stem) | Disruption of the BBB (abnormal ZO-1) |
|---|---|---|---|---|---|
| APOE 3/3 TLR4 + | 27y M | Control | — | — | + |
| APOE 3/3 TLR4 + | 27y M | Control | — | — | — |
| APOE 3/3 TLR4 + | 28y M | MC | Frontal, hippocampus | — | + |
| APOE 3/3 TLR4 + | 29y M | MC | — | — | + |
| APOE 3/3 TLR4 + | 30y M | MC | — | — | + |
| APOE 3/3 TLR4 + | 31y M | MC | Frontal diffuse plaques | — | + |
| APOE 3/3 TLR4 + | 34y M | MC | frontal | Dorsal nucleus vagus, locus ceruleus, medulla | + |
| APOE 3/3 TLR4 + | 35y M | MC | — | Brain stem nuclei | + |
| APOE 3/3 TLR4 + | 37y M | MC | frontal | — | + |
| APOE 3/3 TLR4 + | 38y M | MC | — | — | + |
| APOE 3/3 TLR4 + | 40y M | Control | — | — | + |

| Genotype (APOE TLR4) | Age/gender | Residency | Aβ42 immunoreactivity (OB, frontal, hippocampus) | α-synuclein immunoreactivity (OB, brain stem) | Disruption of the BBB (abnormal ZO-1) |
|---|---|---|---|---|---|
| APOE 3/3 TLR4 + | 45y M | MC | Frontal, hippocampus | midbrain | + |
| APOE 3/3 TLR4 + | 45y M | MC | — | — | + |

Abbreviations: Aβ42, beta amyloid; APOE, apolipoprotein E; BBB, blood-brain barrier; HLA-DR, human leukocyte antigen-DR; MC, Mexico City; OB, olfactory bulb; TLR, toll-like receptor; ZO-1, zonula occludens-1.

**Table 3** RT-PCR sample results from Control vs MC lung, CNS, and PNS tissues, and their statistical significance.

| Anatomical region and gene | Controls | Mexico City residents | Statistical significance |
|---|---|---|---|
| COX2 lung[a] | 15.9 ± 6.7 $x10^6$ | 42.3 ± 7.4 $x10^6$ | .015 |
| IL-1β lung[a] | 3.08 ± 1.87 $x10^6$ | 4.51 ± 2.6 $x10^6$ | .60 |
| COX2 OB[a] | 12.9 ± 3.0 x $10^5$ | 38.7 ± 5.5 x $10^5$ | .0002 |
| IL-1β OB[a] | 3.4 ± 0.8 x $10^4$ | 7.7 ± 1.0 x $10^4$ | .003 |
| CD14 OB[b] | 0.01 ± 0.001 | 0.04 ± 0.01 | .04 |
| COX2 frontal[a] | 2.6 ± 0.4x $10^5$ | 5.0 ± 0.7 x $10^5$ | .008 |
| IL-1β frontal[a] | 0.6 ± 0.2 $x10^4$ | 6.2 ± 1.3 $x10^4$ | .0002 |

| Anatomical region and gene | Controls | Mexico City residents | Statistical significance |
|---|---|---|---|
| COX2 hippocampus[a] | 1.9 ± 0.5x $10^5$ | 1.6 ± 8.7 x $10^5$ | .1 |
| IL-1β hippocampus[a] | 1.8 ± 0.2 x$10^4$ | 3.0 ± 0.5 x$10^4$ | .06 |
| COX2 substantia nigrae[a] | 0.16 ± 0.06 | 0.97 ± 0.2 | .03 |
| IL-1β substantia nigrae[b] | 0.01 ± 0.005 | 0.09 ± 0.03 | .06 |
| CD14 substantia nigrae[b] | 0.02 ± 0.005 | 0.03 ± 0.007 | .7 |
| COX2 periaqueductal gray[b] | 0.10 ± 0.03 | 0.45 ± 0.12 | .12 |
| IL-1β periaqueductal gray[b] | 0.009 ± 0.003 | 0.07 ± 0.02 | .09 |
| COX2 left vagus[b] | 0.65 ± 0.18 | 2.68 ± 0.82 | .03 |
| COX2 right vagus[b] | 0.43 ± 0.09 | 3.68 ± 0.8 | .0002 |
| IL1β left vagus[b] | 0.1 ± 0.03 | 1.3 ± 0.73 | .06 |
| IL1β right vagus[b] | 0.15 ± 0.09 | 0.87 ± 0.53 | .66 |
| CD14 left vagus[b] | 0.07 ± 0.01 | 0.79 ± 0.41 | .01 |
| CD14 right vagus [b] | 0.05 ± 0.01 | 0.31 ± 0.1 | .02 |

Abbreviations: CNS, central nervous system; MC, Mexico City; OB, olfactory bulb; PNS, peripheral nervous system; RT-PCR, real-time polymerase chain reaction.

The amount of COX2, IL-1β and CD14 cDNA in each sample was normalized to the amount of GAPDH cDNA, yielding an index (molecules per femtomol[a] or molecules/uEq[b] GAPDH rRNA) proportional to the relative abundance of each mRNA in each sample.

**Table 4** Results of APOE and TLR4 genotyping, Aβ42 and α-synuclein immunoreactivity by

immunohistochemistry in Control and Mexico City subjects with the APOE 4 allele.

| Genotype | Age | Gender | Residency | Aβ 42 | α-synuclein |
|---|---|---|---|---|---|
| E4/E4 TLR4+ | 32 | F | MC | Olfactory bulb, blood vessels, and cortical neurons | + substantia nigrae, mesencephalic V |
| E3/E4 TLR4+ | 15 | M | MC | Cortical neurons and diffuse plaques | — |
| E3/E4 TLR4– | 20 | M | MC | Olfactory bulb, blood vessels, and cortical neurons | — |
| E3/E4 TLR4+ | 22 | M | MC | Cortical neurons and diffuse plaques | — |
| E3/E4 TLR4+ | 25 | M | MC | Olfactory bulb and cortical neurons | + olfactory bulb |
| E3/E4 TLR4+ | 32 | M | MC | Cortical neurons | — |
| E3/E4 TLR4+ | 34 | M | MC | Cortical neurons | — |
| E3/E4 TLR4+ | 36 | M | MC | Olfactory bulb, cortical neurons, diffuse and mature plaques | — |
| E3/E4 TLR4+ | 36 | F | Control | Plaques diffuse and mature | — |
| E3/E4 TLR4+ | 44 | M | Control | — | — |
| E3/E4 TLR4+ | 45 | M | Control | Olfactory bulb and cortical neurons | — |

Abbreviations: APOE, apolipoprotein E; MC, Mexico City; RT-PCR, real-time polymerase chain reaction; TLR, toll-like receptor.

**Table 5** Distribution of subjects with expression of Aβ42 as a function of age and residency.

| Groups/number of cases | Aβ42 Number of cases IHC+ | % of cases | Average age |
|---|---|---|---|
| Controls < 25 y APOE 3/3 N: 6 | 0 | 0 | 16.33 ± 3.09 |
| Controls > 25 y APOE 3/3 N:3 | 0 | 0 | 31.3 ± 4.3 |
| MC E2 or E3 < 25 y N:17 | 10 | 58.82 | 17.41 ± 1.51 |
| MC E2 or E3 > 25 y N:10 | 8 | 80 | 35.2 ± 1.9 |
| MC E4 N:8 | 8 | 100 | 27 ± 7.5 |
| Controls E4 N:3 | 2 (36 y, 45 y) | 66 | 41.67 ± 2.85 |

Abbreviation: APOE, apolipoprotein E; IHC, immunohistochemistry; MC, Mexico City.

**Table 6** Distribution of subjects with α-synuclein as a function of age and residency.

| Groups/number of cases | α-synuclein Number of cases IHC+ | % cases | Average age |
|---|---|---|---|
| Controls < 25 y APOE 3/3 N: 6 | 0 | 0 | 16.33 ± 3.09 |
| Controls > 25 y APOE 3/3 N:3 | 0 | 0 | 31.3 ± 4.3 |
| MC E2 or E3 < 25 y N:17 | 4 | 23.5 | 17.41 ± 1.51 |
| MC E2 or E3 > 25 y N:10 | 3 | 30 | 35.2 ± 1.9 |
| MC E4 N:8 | 2 | 25 | 27 ± 7.5 |

| Groups/number of cases | α-synuclein Number of cases IHC+ | % cases | Average age |
|---|---|---|---|
| Controls E4 N:3 | 0 | 0 | 41.67 ± 2.85 |

Abbreviation: APOE, apolipoprotein E; MC, Mexico City.

Show Details

**SAGE Knowledge**

Whole book

Build the Brain for Reading Grades 4â€ 12

Show Details

View More

## Also from Sage

### CQ Library

Elevating debate

### Sage Data

Uncovering insight

### Sage Business Cases

Shaping futures

### Sage Campus

Unleashing potential

### Sage Knowledge

Multimedia learning resources

### Sage Research Methods

Supercharging research

### Sage Video

Streaming knowledge

### Technology from Sage

Library digital services